Received: 23 July 2018 | Revised: 3 December 2018 | Accepted: 6 December 2018

DOI: 10.1111/pce.13500

ORIGINAL ARTICLE

WILEY Plant, Cell & Environment

# Contrasting stomatal sensitivity to temperature and soil drought in mature alpine conifers

Richard L. Peters[1,2] | Matthias Speich[1,3] | Christoforos Pappas[4,5] | Ansgar Kahmen[2] | Georg von Arx[1] | Elisabeth Graf Pannatier[1] | Kathy Steppe[6] | Kerstin Treydte[1] | Ana Stritih[7] | Patrick Fonti[1]

[1] Forest Dynamics, Landscape Dynamics and Forest Soils and Biogeochemistry, Swiss Federal Research Institute for Forest, Snow and Landscape Research WSL, Birmensdorf CH-8903, Switzerland

[2] Department of Environmental Sciences–Botany, Basel University, Basel CH-4056, Switzerland

[3] Department of Environmental Systems Science, ETH Zurich, Zurich CH-8092, Switzerland

[4] Département de géographie and Centre d'études nordiques, Université de Montréal, Montréal, Quebec, Canada

[5] Faculty of Environmental Sciences, Czech University of Life Sciences Prague, Prague, Czech Republic

[6] Laboratory of Plant Ecology, Department of Plants and Crops, Faculty of Bioscience Engineering, Ghent University, Ghent B-9000, Belgium

[7] Institute for Landscape and Spatial Development, Planning of Landscape and Urban Systems (PLUS), ETH Zurich, Zürich CH-8093, Switzerland

**Correspondence**
R. L. Peters, Swiss Federal Research Institute for Forest, Snow and Landscape Research WSL, Zürcherstrasse 111, Birmensdorf CH-8903, Switzerland.
Email: richard.peters@wsl.ch

**Funding information**
Stavros Niarchos Foundation; ETH Zurich Foundation; Swiss National Science Foundation, Grant/Award Number: P2EZP2_162293, P300P2_174477 and 150205

## Abstract

Conifers growing at high elevations need to optimize their stomatal conductance ($g_s$) for maximizing photosynthetic yield while minimizing water loss under less favourable thermal conditions. Yet the ability of high-elevation conifers to adjust their $g_s$ sensitivity to environmental drivers remains largely unexplored.

We used 4 years of sap flow measurements to elucidate intraspecific and interspecific variability of $g_s$ in *Larix decidua* Mill. and *Picea abies* (L.) Karst along an elevational gradient and contrasting soil moisture conditions. Site- and species-specific $g_s$ response to main environmental drivers were examined, including vapour pressure deficit, air temperature, solar irradiance, and soil water potential.

Our results indicate that maximum $g_s$ of *L. decidua* is >2 times higher, shows a more plastic response to temperature, and down-regulates $g_s$ stronger during atmospheric drought compared to *P. abies*. These differences allow *L. decidua* to exert more efficient water use, adjust to site-specific thermal conditions, and reduce water loss during drought episodes.

The stronger plasticity of $g_s$ sensitivity to temperature and higher conductance of *L. decidua* compared to *P. abies* provide new insights into species-specific water use strategies, which affect species' performance and should be considered when predicting terrestrial water dynamics under future climatic change.

KEYWORDS

conifers, high-elevation forests, hydraulic plasticity, interspecific and intraspecific variability, *Larix decidua*, *Picea abies*, sap flow, stomatal conductance, transpiration

**Abbreviations:** $A_L$, leaf area; $A_S$, sapwood area; $C_p$, heat capacity of air; $D$, vapour pressure deficit; DBH, stem diameter at breast height (1.3 m); $E$, transpiration; $F_d$, sap flux density; $g_s$, stomatal conductance (standardized to $A_L$); $g_s/g_{s.max}$, stomatal conductance relative to the maximum (99th quantile); $g_{sap}$, crown conductance (standardized to $A_S$); $g_{sap.int}$, intercept of the linear relationship between $\psi_{soil}$ and $g_{sap}/g_{sap.max}$; $g_{sap}/g_{sap.max}$, crown conductance relative to the maximum (99th quantile); $g_{sap.ref}$, reference conductance when $D = 1$ kPa; $K$, $\Delta T$ standardized for $\Delta T_{max}$; $R_g$, solar irradiance; $RH$, relative humidity; $T_a$, air temperature; $T_s$, soil temperature; $W_u$, whole-tree water flux; $\gamma$, psychrometric constant; $\Delta T$, temperature difference between heated and unheated sap flow probe; $\Delta T_{max}$, temperature difference during zero-flow conditions; $-\delta$, slope coefficient of the power function between $T_a$ and $g_{sap}$; $\theta$, volumetric soil water content; $\Lambda$, slope coefficient of the linear relationship between $\psi_{soil}$ and $g_{sap}/g_{sap.max}$; $\lambda$, latent heat of vaporization; $\rho$, air density; $\psi_{soil}$, soil water potential

  

## 1 | INTRODUCTION

The biogeographical distribution of coniferous trees extends across a wide range of contrasting environmental conditions, from the Arctic Circle to the equator and Southern Hemisphere (Farjon & Filer, 2013). Although many factors affect the distribution of tree species (see Walthert & Meier, 2017; Zimmermann, Edwards, Graham, Pearman, & Svenning, 2010), conifers often dominate at high elevations where low temperatures and short growing seasons severely limit growth and survival (Bannister & Neuner, 2001; Körner, 2012). For example, it is very common to find conifers at the upper treeline with growing season temperatures as low as 5.5–7.5°C (Körner & Paulsen, 2004). Under such temperature-limited conditions, growth is known to be highly sensitive to ongoing climate change (Beniston, 2003; IPCC, 2013; Soja et al., 2007). Recent studies indicated that warmer and drier conditions in temperature-limited ecosystems (at high elevations and latitudes) are altering the forest composition and the timing and duration of both primary and secondary growth (e.g., Allen et al., 2010; Esper & Schweingruber, 2004; Meier, Lischke, Schmatz, & Zimmermann, 2012; Peters, Klesse, Fonti, & Frank, 2017; Rigling et al., 2013; Steltzer & Post, 2009). Subsequently, these changes have consequences for the terrestrial biogeochemical cycles and the global climate system (Bonan, 2008; Myneni et al., 2001).

When growing under a wide range of climatic conditions, trees need to optimize carbon assimilation and its use, that is, the formation and maintenance of woody and nonwoody tissues (see Fatichi, Leuzinger, & Körner, 2014; Körner, 2012; Maseyk et al., 2008; Rossi et al., 2008). Both the processes of producing carbohydrates (via photosynthesis; Nobel, 2009) and the generation of turgidity within the cambium required for growth (Lockhart, 1965) depend on the way a tree regulates the flow of water through the soil–plant–atmosphere continuum (Damour, Simonneau, Cochard, & Urban, 2010; De Schepper & Steppe, 2010; Mencuccini, 2003; Tuzet, Perrier, & Leuning, 2003). Conifers thus underwent strong selective pressure to develop specialized ways to regulate their internal hydraulics (Anderegg et al., 2016; Brodribb, Mcadam, Jordan, & Martins, 2014; Klein, 2014). Main mechanisms for controlling tree water use usually include anatomical adjustments of the water conducting xylem (e.g., Bouche et al., 2014; Mayr, Hacke, Schmid, Schienbacher, & Gruber, 2006) and the optimization of the stomatal conductance ($g_s$) to quickly respond to varying environmental conditions (Hetherington & Woodward, 2003; Lin et al., 2015). The regulation of $g_s$ sensitivity is crucial under temperature-limited conditions, as transpiration has to be optimized for minimal water loss during cold spells and under frozen soil conditions (Mayr, 2007) and maximum photosynthetic yield during the short vegetative season (i.e., to produce ample sugars for frost damage protection; see Körner, 2012; Lintunen et al., 2016). This optimization is supported by observations of increasing maximum $g_s$ with increasing elevation (Körner, 2012) and deciduous conifers like *Larix decidua* Mill. (with a shorter growing season) showing an overall higher conductance than evergreen *Picea abies* (L.) Karst. and *Pinus cembra* L. (Anfodillo et al., 1998). However, although the species-specific difference in the sensitivity of $g_s$ to temperature could be relevant for optimizing tree water use under temperature-limited conditions, most studies have focussed on stomatal responses to atmospheric and soil droughts (e.g., Arneth et al., 1996; Day, 2000; Leo et al., 2014; Lindroth, 1985; Wieser, Leo, & Oberhuber, 2014).

Under rapidly changing climatic conditions, the future performance and occurrence of a species depends on its plasticity (Valladares et al., 2014), that is, the ability to adjust physiological functioning under a wide range of growing conditions. This also holds for tree water use, because species survival in persistent warmer and drier conditions largely depends upon the plastic adjustment of its hydraulic functioning (e.g., Cordell, Goldstein, Mueller-Dombois, Webb, & Vitousek, 1998; Körner, Bannister, & Mark, 1986; López et al., 2013; Martínez-Vilalta et al., 2009). Thus, there has been interest in comparing interspecific and intraspecific shifts in $g_s$ response to vapour pressure deficit ($D$) at sites with contrasting climatic conditions (e.g., Poyatos et al., 2007). For example, a study by Grossiord et al. (2017) on conifers growing in a semiarid climate found a reduced stomatal sensitivity to $D$ when exposed to persistent warming. Although conifers growing at different thermal conditions (e.g., along elevational gradients) show a uniform $g_s$ response to $D$ (Mayr, 2007), their ability to adjust their $g_s$ response to air temperature ($T_a$) and solar radiance ($R_g$) might be crucial for optimizing tree water use (Buckley & Mott, 2013; Livingston & Black, 1987). For example—due to the shorter growing season, low temperatures, and reduced partial pressure of $CO_2$ at higher elevations (Körner, 2012)—a strategy to optimize carbon assimilation might allow higher $g_s$ at low temperatures, despite thermal conditions being less favourable for photosynthetic activity (Damour et al., 2010; Wieser, 2007). In addition, due to low drought stress conditions (Körner, 2012), high-elevation conifers could reduce $g_s$ sensitivity to $R_g$, where incomplete stomatal closure during the night allows for a faster supply of water to the leaves at sunrise (e.g., Daley & Phillips, 2006). Yet the ability of high-elevation conifers to adjust their $g_s$ response to these environmental drivers in the context of a warming atmosphere remains largely unexplored.

In this study, we investigated the stomatal regulation of *P. abies* and *L. decidua* and its plasticity along an elevational gradient in the central Swiss Alps that stretches up to the species' upper distribution limits (Ellenberg & Leuschner, 2010) and shows a genetically well-mixed population (King, Gugerli, Fonti, & Frank, 2013). In addition to a thermal gradient, with a persistent difference in mean growing season temperature of up to 3.2°C, trees at contrasting soil moisture conditions were also monitored. At five different sites, we installed thermal dissipation probes to obtain 4 years of sap flow measurements, including a strong drought event in the summer of 2015. The sap flow measurements were used to calculate $g_s$ and analyse its sensitivity to environmental conditions at each site. We hypothesize that drought sensitive *P. abies* (Anfodillo et al., 1998; Ježík et al., 2015) will show a stronger down-regulation of its stomatal conductance to increasing $D$ and increasing drought (by measuring soil water potential, $\psi_{soil}$) compared to *L. decidua*. Additionally, for each species, we quantified the sensitivity and plasticity of $g_s$ response functions to multiple environmental drivers (including $D$, $\psi_{soil}$, $T_a$, and $R_g$) across the elevational gradient, where we specifically differentiate between soil and atmospheric drought (Klein, Yakir, Buchmann, & Grünzweig, 2014; Tatarinov et al., 2016). As pioneer species are expected to show higher plasticity (Barigah et al., 2006; Sultan, 2000), we hypothesize that the pioneer *L. decidua* (Gower & Richards, 1990) will show a more plastic adjustment of its $g_s$ response to environmental drivers compared to the late-successional species *P. abies*. The analysis of the stomatal behaviour of high-elevation conifers offers a unique perspective on the plasticity of their

hydraulic functioning and provides insights into their ability to optimize water use under future climatic conditions.

## 2 | MATERIALS AND METHODS

### 2.1 | Site description

The studied trees are located at several sites situated within the Lötschental valley in the Swiss Alps (46°23′40″N, 7°45′35″E; Figure 1a). The valley is characterized by steep slopes (>60%) and covered with a mixed forest of naturally occurring evergreen *P. abies* and deciduous *L. decidua*. Average forest stand density at the sites is 401 ± 144 trees ha$^{-1}$, with an average tree age of 173 ± 45 years, diameter at breast height (DBH) of 45 ± 4 cm and canopy height of 22 ± 4 m (Peters et al., 2017). Soils are formed from calcareous-free substrate, including moraines and crystalline bedrock (gneiss and granite) from the Aar massif. Several different soil types were classified at the valley slope, including Leptosol, Cambisol to Podzol. Soil texture consists of 10 ± 4% clay, 56 ± 10% sand, and 35 ± 8% silt content and with fine soil bulk density of 0.77 ± 0.42 g cm$^{-3}$. At the valley bottom with wetter soil conditions, organic soils (Histosol) with low bulk density (0.19 ± 0.07 g cm$^{-3}$) occur. Long-term mean annual total precipitation and mean annual air temperature in the valley exceeds 800 mm and approximates 5.7°C, respectively (King, Fonti, Nievergelt, Büntgen, & Frank, 2013).

Sap flow and environmental conditions were continuously monitored from April 2012 to October 2015 at five sites distributed across a thermal and moisture gradient. Four of these sites are situated along an elevational gradient on a south-facing slope with a 300 m interval from the valley bottom at 1,300 m a.s.l. to the treeline at ~2,200 m a.s.l. The site at the treeline, close to the distribution limit of *L. decidua* (hereafter referred as S22, where S indicates the south-facing slopes), showed a mean growing season (May–October) air temperature of 8.3°C (covering 2012–2015). The site at 1,900 m a.s.l. (S19), corresponding to the distribution limit of *P. abies*, showed slightly warmer conditions with a mean growing season air temperature of 9.2°C. The two sites at 1,600 (S16) and 1,300 m a.s.l. (N13, where N indicates the north-facing slopes) experienced sequentially drier and warmer conditions, with a mean growing season air temperature of 10.4°C and 11.5°C, respectively. A fifth contrasting wet site was established at the valley bottom close to the Lonza river, providing constant water saturation at 70-cm soil depth (N13W), with a slightly cooler mean growing season air temperature of 10.4°C.

### 2.2 | Environmental measurements

Radiation-shield covered sensors were installed at each site on a central tower (~2.5 m above the ground) within the canopy to measure air temperature ($T_a$ [°C]) and relative humidity (*RH* [%]; Onset, USA, U23–002 Pro) with a 15-min temporal resolution. Vapour pressure deficit (*D* [kPa]) was calculated from $T_a$ and *RH* (WMO, 2008). Soil temperature ($T_S$ [°C]) was recorded at each site with an hourly resolution at a depth of 10 cm (Onset, USA, TdbiT). At N13, solar irradiance ($R_g$ [W m$^{-2}$]) was measured with 15-min resolution using a microstation (Onset, USA, H21–002 Micro Station) and pyranometer (Onset, USA, S-LIB-M003) positioned in an open field. For the other sites, $R_g$ measurements were adjusted for aspect and topographic shading after Schulla (2015).

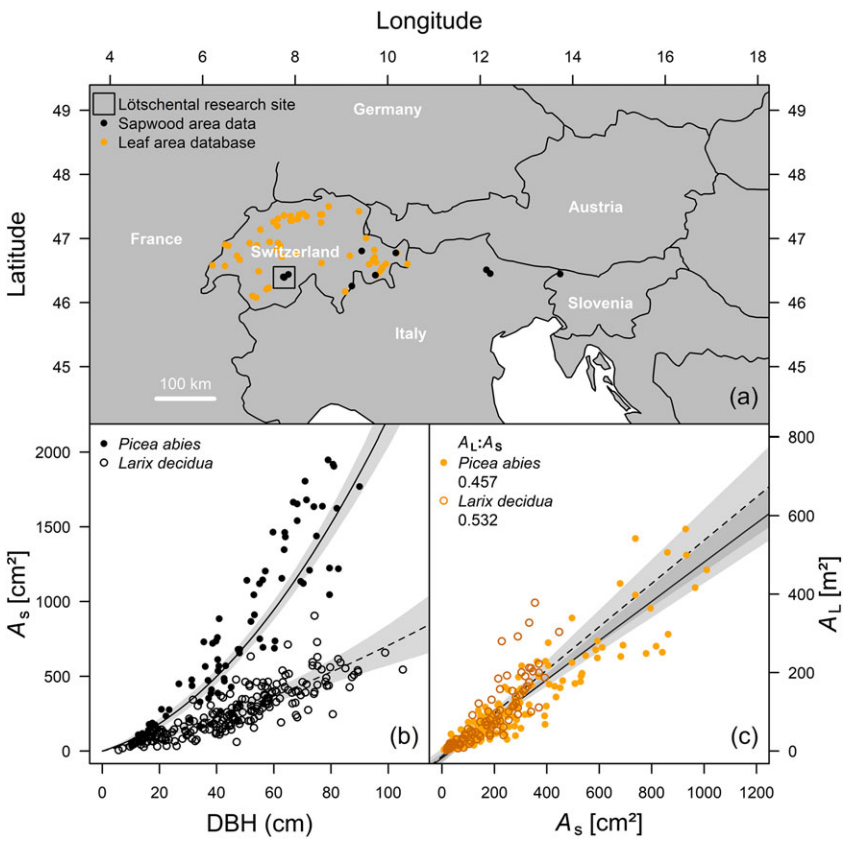


**FIGURE 1** Research site, sampling locations, and derived allometric relationships. (a) Location of the Lötschental research site, trees sampled in the leaf area database, and trees for which the sapwood area was measured. (b) Relationship between diameter at breast height (DBH) and sapwood area ($A_S$) and (c) relationship between projected leaf area ($A_L$) and modelled $A_S$ (using DBH measurements and the relationship presented in b) for the respective $A_L$:$A_S$ values. Lines indicate model fits for *Larix decidua* (dotted) and *Picea abies* (solid). Grey areas present the Bayesian credible interval of the fitted function (see Gelman & Hill, 2007)

Calculations for topographic shading were based on the digital height model DHM25 (Swiss Federal Office of Topography Swisstopo).

Soil volumetric water content was measured hourly with five sensors at 10- and 70-cm depth at each site ($\theta$ [%]; Decagon, USA, EC-5). At the same depth, soil water potential was also measured ($\psi_{soil}$ [MPa]; Decagon, USA, MPS-2) for 2015. These measurements were used for establishing soil water retention curves using the van Genuchten model (van Genuchten, 1980), where the saturated water content was established according to Teepe, Dilling, and Beese (2003); see Table S1). This allowed retrospective determination of $\psi_{soil}$ for the entire monitoring period. The water content at permanent wilting point and field capacity was visually determined to normalize $\theta$ to relative extractable water (in %; Granier, Bréda, Biron, & Villette, 1999). The wettest conditions from both depths for $\theta$ and $\psi_{soil}$ were used to represent the site conditions.

Daily precipitation was obtained from the nine nearest weather stations (6- to 43-km distance to the transect, including Adelboden, Blatten, Grächen, Montana, Jungfraujoch, Sion, Ulrichen, Visp, and Zermatt; Federal Office of Meteorology and Climatology MeteoSwiss). The environmental measurements at each site were quality controlled and the few sporadic data gaps were filled by linear interpolation or by using a regression approach with a stiff cubic spline on data from other sites and hourly averaged (using the *mgcv* package in R software version 3.2.00, R development core team 2013).

## 2.3 | Physiological measurements and conductance calculations

At every site, three mature trees per species (a total of 15 *L. decidua* and 12 *P. abies* trees; Table 1) were instrumented with commercially available thermal dissipation probes (Granier, 1985; Tesaf, University of Padova, Italy) to estimate sap flux density ($F_d$ [g $H_2O$ $cm^{-2}$ sapwood area $hr^{-1}$]). Two 2-cm long probes were radially inserted into the xylem (below the cambium), with a vertical distance of 10 cm on the slope-facing side of the stem at ~1.6-m height. The temperature difference between the probes ($\Delta T$ [°C]) was recorded with 15-min resolution on a data logger (Campbell Scientific, USA, CR1000). The normalized difference (denoted as unitless $K$ [–]) between measured $\Delta T$ and zero sap flow conditions ($\Delta T_{max}$; Lu, Urban, & ZHao, 2004) was calculated. $F_d$ was calculated with $K$ by using the data-processing method described in Peters et al. (2018), correcting for the probe in nonconductive xylem, applying a species-specific calibration, dampening correction and environmental dependent determination of zero-flow conditions. The internal tree water status was monitored at the dry site (N13) by measuring leaf water potential ($\psi_{leaf}$ [MPa]) on three mature trees per species for which the crown was reachable by pole pruner. During three sampling campaigns, we measured pre-dawn $\psi_{leaf}$ (<6:00 CET on 19-04-2014, 21-07-2015, and 24-09-2015), whereas we measured weekly midday $\psi_{leaf}$ (11:00–15:00 CET) during the 2015 growing season (June–September). Measurements were performed by using a Scholander pressure chamber (Boyer, 1967) on four twigs (~5 cm) per tree.

Sapwood thickness was measured from two increment wood cores (using an increment borer; Haglöf, Sweden) taken perpendicular to the slope at breast height (~1.3 m) from the monitored trees (based on discolouration for *L. decidua* and translucence for *P. abies*). $F_d$ was multiplied by the sapwood area ($A_S$ [$cm^2$]) to obtain whole-tree water flux ($W_u$ [kg $H_2O$ $h^{-1}$]; see Table 1), where *P. abies* has a mean $A_S$ of 710 $cm^2$ (with exceptionally high values for N13W), and *L. decidua* has a mean $A_S$ of 307 $cm^2$. Whole-tree water flux was then used to estimate transpiration per unit of leaf area (i.e., $E$ [g $H_2O$ $m^{-2}$ leaf area $hr^{-1}$]) by using

**TABLE 1** Characteristics of trees instrumented with thermal dissipation probes

| Species | Site | Elevation (m a.s.l.) | Tree ID | Age (year) | DBH (cm) | Height (m) | $A_S$ ($cm^2$) | Max. $W_u$ (kg $hr^{-1}$) |
|---|---|---|---|---|---|---|---|---|
| *Larix decidua* | N13 | 1,300 | N13Bd_L1 | 131 | 29.5 | 20.1 | 105 | 10.8 |
| | | | N13Bd_L2 | 128 | 32.0 | 18.5 | 142 | 2.7 |
| | | | N13Ad_L4 | 131 | 30.8 | 18.7 | 125 | 8.0 |
| | N13W | 1,300 | N13WAd_L1 | 148 | 78.0 | 27.7 | 464 | 16.4 |
| | | | N13WBd_L2 | 164 | 89.3 | 33.3 | 541 | 19.4 |
| | | | N13WBd_L3 | 134 | 52.0 | 25.7 | 304 | 9.4 |
| | S16 | 1,600 | S16Bd_L1 | 371 | 75.2 | 31.5 | 629 | 5.7 |
| | | | S16Ad_L1 | 69 | 38.5 | 24.5 | 251 | 17.3 |
| | | | S16Ad_L4 | 69 | 41.5 | 23.8 | 369 | 8.7 |
| | S19 | 1,900 | S19Ad_L1 | 200 | 48.0 | 23.7 | 300 | 8.7 |
| | | | S19Ad_L3 | 170 | 35.5 | 26.3 | 224 | 6.5 |
| | | | S19Bd_L1 | 326 | 48.7 | 22.4 | 208 | 6.6 |
| | S22 | 2,200 | S22Ad_L1 | 269 | 47.0 | 17.8 | 292 | 5.2 |
| | | | S22Ad_L2 | 280 | 55.7 | 17.2 | 434 | 15.7 |
| | | | S22Ad_L3 | 295 | 45.5 | 16.6 | 218 | 7.1 |
| *Picea abies* | N13 | 1,300 | N13Ad_S1 | 90 | 30.7 | 14.5 | 210 | 3.0 |
| | | | N13Ad_S2 | 93 | 48.1 | 19.8 | 680 | 17.6 |
| | | | N13Bd_S3 | 87 | 37.0 | 19.2 | 473 | 12.3 |
| | N13 W | 1,300 | N13WAd_S1 | 85 | 81.0 | 29.5 | 1,905 | 49.1 |
| | | | N13WAd_S2 | 81 | 62.8 | 33.5 | 1,155 | 23.6 |
| | | | N13WBd_S3 | 109 | 80.7 | 33.6 | 1,918 | 31.0 |
| | S16 | 1,600 | S16Bd_S4 | — | 45.3 | 21.5 | 257 | 10.1 |
| | | | S16Ad_S2 | 62 | 38.2 | 25.3 | 411 | 4.8 |
| | | | S16Bd_S2 | 461 | 56.2 | 23.5 | 315 | 5.1 |
| | S19 | 1,900 | S19Bd_S3 | 245 | 37.2 | 21.2 | 353 | 2.2 |
| | | | S19Ad_S2 | 137 | 34.1 | 25.0 | 161 | 23.5 |
| | | | S19Bd_S2 | 229 | 47.5 | 24.5 | 680 | 4.6 |

*Note*. Age and sapwood area ($A_S$) were determined using increment core measurements. Additionally, the maximum water flux ($W_u$) measured during the monitoring period is provided.

allometric relationships between $A_S$ [cm$^2$] and total projected needle area ($A_L$ [m$^2$]; Figure 1b,c). To generate a robust relationship between DBH and $A_S$, over 450 trees were measured across the alpine range (Figure 1b; see Table S2). Species-specific allometric relationships of DBH-$A_S$ were then used together with a leaf area database (constructed with the measurements from Burger, 1953), recording $A_L$ and DBH, to establish $A_L$:$A_S$ values (Figure 1c; Tyree & Zimmermann, 2002). To account for the delay between $E$ and $F_d$, the mean difference between the time of sunrise and the onset of $F_d$ (15-min resolution) was calculated to shift back $F_d$ to represent $E$. The timing of sunrise was defined every day as the time when $R_g$ exceeds 10 W m$^{-2}$. The onset of $F_d$ was determined when a persistent increase in $F_d$ occurred after 3:00 a.m. Finally, we made use of weekly observations of phenological stages performed from 2008 untill 2011, to remove periods when *L. decidua* did not have full foliage (Moser et al., 2010; see Figure S1).

## 2.4 | Crown and stomatal conductance and their response to environmental drivers

Both crown conductance ($g_{sap}$ [g $H_2O$ m$^{-2}$ sapwood area s$^{-1}$ kPa$^{-1}$]) and stomatal conductance ($g_s$ [mm s$^{-1}$]) were calculated for all individuals. We complemented the $g_s$ calculation with $g_{sap}$, as the latter is less dependent upon model assumptions when comparing species-specific differences. We determined $g_{sap}$ by using $D$ and $F_d$ (adopted from Meinzer et al., 2013 and Pappas et al., 2018):

$$g_{sap} = \frac{(F_d{}^*10000/3600)}{D}. \quad (1)$$

In order to minimize the effect of stem hydraulic capacitance (see Braun, Schindler, & Leuzinger, 2010), only peak-of-the-day hourly values of $g_{sap}$ were considered. Peak-of-the-day was defined as the hours when $R_g$ > 500 W m$^{-2}$. Next, the hourly $g_{sap}$ values were standardized to the individual specific 99th quantile of the time-series ($g_{sap.max}$), to correct for absolute difference in conductance. The relative hourly crown conductance values ($g_{sap}/g_{sap.max}$) were averaged per site and species and aggregated to daily mean values. Species-specific $g_{sap}$ responses to atmospheric drought (approximated with $D$) and soil drought (approximated with $\psi_{soil}$) were analysed for periods when other factors were less limiting. For the response of $g_{sap}$ to $D$, days were selected with $T_a$ > 12°C, $\theta$ > 60% and precipitation <10 mm day$^{-1}$, whereas for $\psi_{soil}$, we selected days with $D$ < 0.8 kPa instead of $\theta$. To explain responses in $g_{sap}$ to $D$ and $\psi_{soil}$, we fitted linear functions as $g_{sap.ref} - \delta * \ln D$ ($g_{sap.ref}$ is the reference conductance when $D$ = 1 kPa; see Oren et al., 1999) and $g_{sap.int} + \Lambda * \psi_{soil}$, respectively. Linear-mixed effect modelling was applied, where the individual tree is considered as the random effect while accounting for first-order autocorrelation. Due to high variability in $g_{sap}/g_{sap.max}$ at low $\psi_{soil}$ values, the linear function for $\psi_{soil}$ only considers data < −0.2 MPa.

An inversed simplified Penman–Monteith equation was used to calculate $g_s$ (Granier & Loustau, 1994; Monteith, 1965), assuming that conifer forests are aerodynamically well coupled to the atmosphere (Monteith & Unsworth, 2013). Together with the hourly averaged $T_a$, $D$, and $E$ estimates, $g_s$ was calculated according to the following equation (see Note S1):

$$g_s = \frac{\lambda\, E\, \gamma}{\rho\, C_p\, D} \quad (2)$$

where $\lambda$ is the latent heat of vaporization ([J g$^{-1}$]; as a function of $T_a$), $\gamma$ is referred to as the psychrometric constant ([hPa K$^{-1}$]; as a function of air pressure, which is calculated from elevation and $T_a$), $\rho$ is the air density ([kg m$^{-3}$]; as a function of $T_a$ and atmospheric pressure), and $C_p$ is the heat capacity of air ([J kg$^{-1}$ K$^{-1}$]; taken as 1.01 J kg$^{-1}$ K$^{-1}$). The $g_s$ was standardized to the 99th quantile of the individual specific stomatal conductance ($g_{s.max}$), after which hourly $g_s/g_{s.max}$ values were averaged per site and species. A Jarvis-type approach (Jarvis, 1976) was used to analyse the $g_s/g_{s.max}$ response to $D$, $T_a$, $\theta$, $\psi_{soil}$, and $R_g$. We excluded conductance values from rainy days (precipitation >1 mm day$^{-1}$) and with $D$ < 0.1 kPa as these conditions generate unrealistic values (e.g., Phillips & Oren, 1998). For $g_s/g_{s.max}$ values, a bootstrap resampled boundary-line analysis was performed to disentangle when the independent variable is limiting (Chambers, Hinckley, & Hinckley, 1985; Shatar & McBratney, 2004). Within this analysis, a predefined upper quantile was selected when binning the independent variable (e.g., dividing the *x*-axis into classes of a specified size as described in Chambers et al., 1985; Table 2). A bin width of 2% of the total range was used and overlapped by 1% with the previous bin to reduce the effect of uneven distribution of data. For the boundary-line analysis, we excluded conditions where the selected independent variable could show collinearity with other meteorological variables (Table 2). Models were fitted through the upper quantiles to describe the relationship, referred hereafter as response functions (Table 3).

**TABLE 2** Model criteria for the boundary line analysis

| | Variable conditions | | | | | | Bin properties | |
|---|---|---|---|---|---|---|---|---|
| Independent variable | $D$ (kPa) | $T_a$ (°C) | $R_g$ (W m$^{-2}$) | $\Theta$ (-) | $T_s$ (°C) | $\psi_{soil}$ (MPa) | Quantile | Min. *n* |
| Vapour pressure deficit ($D$) | - | >10 | >300 | >0.5 | - | - | 0.95 | 5 |
| Air temperature ($T_a$) | <1.5 | <13 | >300 | >0.5 | - | - | 0.95 | 5 |
| Solar irradiance ($R_g$) | <0.5 | >10 | <800 | >0.5 | - | - | 0.95 | 5 |
| Relative extractable water ($\theta$) | <1.5 | >10 | >300 | >0.8 | - | - | 0.98 | 15 |
| Soil temperature ($T_s$) | <1.5 | - | >300 | >0.5 | <11 | - | 0.95 | 5 |
| Soil water potential ($\psi_{soil}$) | <1.5 | >10 | >300 | - | - | <−0.01 | 0.98 | 15 |

*Note*. Variable conditions are provided for every climatic factor to reduce collinearity. The boundary line is described with non-linear functions by dividing the dataset into bins (segments with a 2% size of the total independent variable range) and a specified quantile was selected per bin (see bin properties). Points where excluded where the bin included less than a specific minimum sample size (see min. *n*). The quantiles and minimum sample size was increased for $\theta$ and $\psi_{soil}$, due to the larger and unequal spread of the data.

**TABLE 3** Selected models used within the boundary-line analysis

| Formula | Description | a | b |
|---|---|---|---|
| $g_s/g_{s.max\text{-}D} = a - bD^{-0.5}$ | An exponential function according to Katul, Palmroth, and Oren (2009). | Asymptote of $g_s/g_{s.max}$ at high $D$ values | Slope |
| $g_s/g_{s.max\text{-}Ta} = 1/(1 + e^{-a(Ta - b)})$ | Instead of applying parabolically shaped functions as proposed by Jarvis (1976), due to the collinearity with $D$ and $g_s$ values approaching zero at low temperatures, a Gompertz function that saturates to 1 $g_s/g_{s.max}$ was used. | Slope of the inflection point (IP) | $T_a$ of the inflection point (IP) |
| $g_s/g_{s.max\text{-}Rg} = 1 - e^{-a(Rg - b)}$ | An adaptation of the model proposed by Price and Black (1989) that allows for night-time activity. | Slope at the $x$-intercept ($g_s/g_{s.max} = 0$) | Shift in $R_g$ for the $x$-intercept ($g_s/g_{s.max} = 0$) |
| $g_s/g_{s.max\text{-}\psi soil} = 1/(1 + a\ e^{(-\psi soil\ b)})$ | As most response functions are based on $\theta$, a new function was used to describe $\psi_{soil}$ response which saturated at 1 $g_s/g_{s.max}$. | The point of the $y$-intercept ($\psi_{soil} = 0$), depending upon the slope | Slope of the inflection point (IP) |

*Note*. Models were selected from literature or constructed to provide parameters that can be interpreted (see *a* and *b*). A general description of the model is provided in addition to the effect of the individual parameters. When relevant, a source is provided.

To elucidate the effect of differences in response function parameters, the species- and site-specific $g_s$ curves were used to model transpiration patterns. We multiplied the site- and species-specific average $g_{s.max}$ with the response functions of $D$, $T_a$, $\psi_{soil}$, and $R_g$ to obtain $g_s$, which was used together with $T_a$, $D$ in Equation (2). To highlight the effect of different response function parameters on daily $E$ dynamics, curves for $T_a$, $D$, and $R_g$ between high and low elevation sites were alternated. The effects of spring and autumn phenological development of *L. decidua* on the resulting $g_s$ were simulated with the models of Murray, Cannell, and Smith (1989) and Delpierre et al. (2009) using daily mean $T_a$ and day length data, respectively. All analyses were performed with the R software (version 3.2.00, R development core team 2013).

## 3 | RESULTS

### 3.1 | Allometry and temporal dynamics of sap flow and transpiration

Species-specific allometric relationships between $A_S$ and DBH were established for *L. decidua* and *P. abies* (Figure 1b). The quadratic function showed a significantly steeper increase in $A_S$ with increasing DBH for *P. abies* ($P < 0.001$; $A_S = 10.76\ \text{DBH} + 0.18\ \text{DBH}^2$) than *L. decidua* ($A_S = 4.78\ \text{DBH} + 0.02\ \text{DBH}^2$). When applying these functions on the leaf area data (covering 59 sites across Switzerland), similar $A_L$:$A_S$ values of 0.457 and 0.532 were found for *P. abies* and *L. decidua*, respectively ($P = 0.265$ using a linear-mixed effect model; Figure 1c; see Table S2).

A substantial time-lag between sunrise and start of $F_d$ was revealed for both *P. abies* and *L. decidua*. No significant difference in delay was found between sites ($P > 0.1$; using a linear-mixed effect model, see Table S3), despite intraspecific differences in height and DBH across the sites (Table 1). *P. abies* showed a significantly longer delay of 2 hr and 45 min, whereas *L. decidua* showed an average delay of 1 hr and 45 min ($P < 0.001$; Table S3). Also, the absolute spread of the delay was higher for *P. abies* (standard error is ~17, against ~12 min delay for *L. decidua*; see Table S3).

Over the 4 years of monitoring sap flow, $E$ was consistently higher for *L. decidua* (Figure 2a) than for *P. abies* (Figure 2b). Additionally, the seasonal pattern of $E$ was more pronounced for *L. decidua* (showing a stronger parabolic shape) and showed stronger differences between sites than for *P. abies* with the highest $E$ at N13 (Figure 2a,b). In July 2015, a strong drought was recorded, resulting in a gradual decrease in $E$ for *L. decidua* at N13 (Figure 2c), whereas *P. abies* showed an even stronger response and paused transpiration at N13 and S16 (Figure 2 d). This drought caused an inverse pattern between N13 and N13W, where N13 showed lower $E$ within July 2015 compared to N13W for both species.

### 3.2 | Species-specific conductance response to environmental conditions

The analysis of *L. decidua* and *P. abies* crown conductance revealed that there is a species-specific difference in their maximum values ($g_{sap.max}$), whereas no significant effect of mean growing season temperature was found (Figure 3; $P > 0.5$, also for $g_s$). *L. decidua* showed a significantly higher mean $g_{sap.max}$ of 261.31 g m$^{-2}$ s$^{-1}$ kPa$^{-1}$ compared to *P. abies* (81.34 g m$^{-2}$ s$^{-1}$ kPa$^{-1}$; $P < 0.001$; using a linear-mixed effect model). This difference was also found for maximum stomatal conductance ($g_{s.max}$), which was significantly higher for *L. decidua* (7.8 mm s$^{-1}$) compared to *P. abies* (with a value of 3.5 mm s$^{-1}$; $P = 0.008$). The calculated $g_{s.max}$ fell within the expected range for gymnosperms (Arneth et al., 1996; Kelliher, Leuning, & Schulze, 1993).

Only the N13 site experienced a large enough variability in $\psi_{soil}$ for addressing species-specific crown conductance response to soil drought (Figure 4). Daily $g_{sap}/g_{sap.max}$ showed a slightly more negative response to $D$ for *L. decidua* (Figure 4a). Significant changes in $-\delta$ and $g_{sap.ref}$ were obtained when using a linear-mixed effect model ($-\delta$ changed by 0.102, $P < 0.001$; $g_{sap.ref}$ change by −0.141, $P < 0.037$). For the response to $\psi_{soil}$, *L. decidua* showed consistently higher $g_{sap}/g_{sap.max}$ values ($g_{sap.ref}$ *L. decidua* > *P. abies*; Figure 4b; $P = 0.051$). The slopes of the linear relationship between $g_{sap}/g_{sap.max}$ and $\psi_{soil}$ did not significantly differ between the two species ($\Lambda$ in Figure 4b). Although less affected by assumptions on delay time and projected

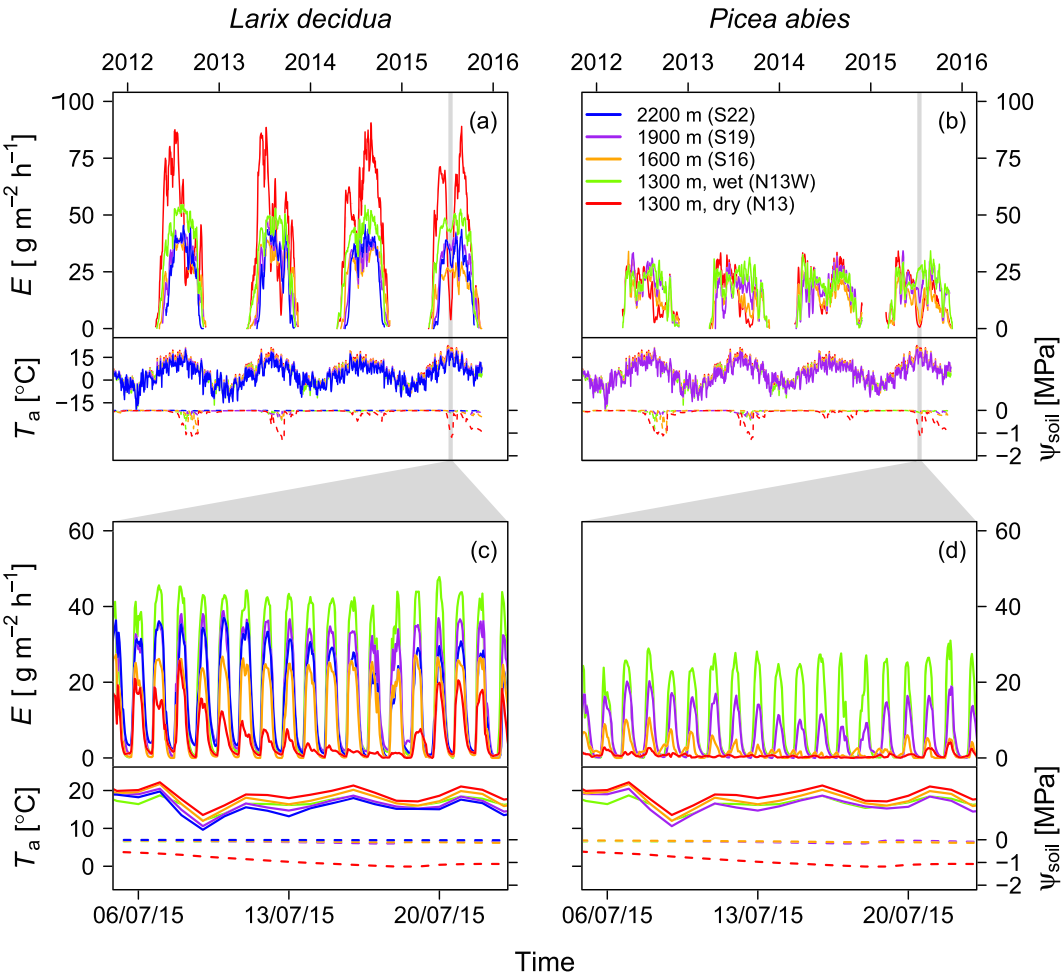


**FIGURE 2** Seasonal and diurnal variations of transpiration ($E$) per site (indicated with elevation in m a.s.l. and specific dry or wet growing conditions) and species. The average $E$ per site and species is presented (in g $H_2O$ $m^{-2}$ leaf area $hr^{-1}$), accounting for the delay time of $F_d$ measurements. Weekly means of daily maximum $E$ are shown for *Larix decidua* (a) and *Picea abies* (b) for the 4 years of monitoring to highlight seasonal variation. Additionally, for a drought period in 2015, a snapshot of hourly $E$ is provided for *L. decidua* (c) and *P. abies* (d). Note that *L. decidua* at the lowest dry site (N13) showed highest $E$ under normal conditions (a), but lowest $E$ during a drought period (c). For every panel, the daily mean $T_a$ and $\psi_{soil}$ measurements are provided

leaf area, daily $g_{sap}$ could not be used at the intradaily time scale to uncover potential interspecific variability in water conductance.

### 3.3 | Intraspecific differences in $g_s/g_{s.max}$ response to environmental conditions

The response of standardized stomatal conductance ($g_s/g_{s.max}$) to $D$, $T_a$, $R_g$, and $\psi_{soil}$ revealed different sensitivities between sites and species (Figure 5). The response of $g_s/g_{s.max}$ to $D$ showed a typical negative exponential behaviour in agreement with theoretical expectations (Roman et al., 2015; Figure 5a,b), with a stronger initial decrease in $g_s/g_{s.max}$ for *L. decidua* than for *P. abies* (Table 4; with $a$ = −0.364 ± 0.051 and $b$ = −0.676 ± 0.084 compared to −0.402 ± 0.071 and −0.753 ± 0.080, respectively). Yet little intraspecific difference in *L. decidua* and *P. abies* response to $D$ was found between the sites, except for the more gradual slope of the function for *L. decidua* trees at S22 (Figure 5a).

The sensitivity of stomatal conductance to $T_a$ showed distinct differences between the species (Figure 5c,d). The fitted Gompertz functions (Table 3), to describe the response of $g_s/g_{s.max}$ to $T_a$, revealed little difference in the inflection point ($T_a$ where the slope of the function is steepest; $b$ parameter in Table 4) between sites for *P. abies* (average of 3.3°C; Figure 5d). On the other hand, *L. decidua* showed changing inflection point temperatures at higher elevation sites, decreasing from 6.5°C to 3.2°C (Figure 5c). The slope of the inflection point did not differ from the 95% confidence interval between the sites (parameter $a$ in Table 4). Although the shift of the inflection points to lower $T_a$ at sites with lower growing season temperature for *L. decidua* did not surpass the inflection point found for *P. abies*, an absolute offset between the species became apparent when considering the higher $g_{s.max}$ values for *L. decidua* (see Figure S2a). Similar differentiation between sites was found when considering $T_s$, although the 95% confidence interval was substantially larger (especially for *P. abies*; see Figure S2b).

The $g_s/g_{s.max}$ response to $R_g$ (Table 3) showed for both species that higher elevation sites appeared to respond more slowly to increasing $R_g$ when considering the slope of the fitted function (parameter $a$ in Table 4), where S19 showed the flattest slope with 0.003–0.004 $W^{-1}$ $m^{-2}$ (Figure 5e,f). Additionally, the response

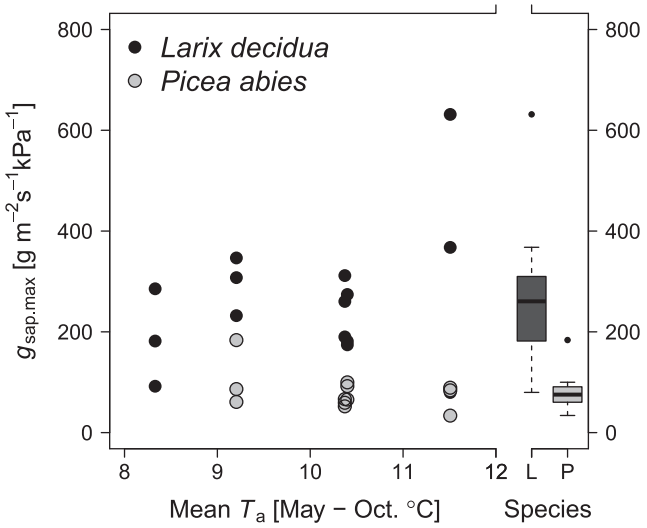


**FIGURE 3** Dependence of maximum crown conductance (99th quantile $g_{sap.max}$) on mean growing season air temperature ($T_a$; from May to October), measured during the 4 years of monitoring, for all individuals (dots) and averaged for both species (L = *Larix decidua* and P = *Picea abies*). Days with precipitation >1 mm and mean daily *D* <0.1 kPa were excluded

functions indicated that higher elevation sites allowed for higher stomatal conductance when $R_g$ approached 0 W m$^{-2}$ (parameter *b* in Table 4). Only the N13 site showed sufficient spread in $\psi_{soil}$ for response curve fitting, where *P. abies* showed a stronger decrease in conductance with increasing $\psi_{soil}$, as was found for $g_{sap}$ (Figure 5g,h).

### 3.4 | Impact of plastic $g_s$ response functions

The impact of differences in the $g_s$ response functions to *D*, $T_a$, and $R_g$ became apparent when modelling daily mean *E* for high- (S22 and S19) and low-elevation (N13) *L. decidua* (Figure 6a,d) and *P. abies* (Table 5). After considering the phenological development (Figure 6c,f), S22 *L. decidua* would transpire up to 5.1 ± 0.7 kg m$^{-2}$ year$^{-1}$ less (4.6 ± 0.7 for S19) if it had a similar $T_a$ response as N13 *L. decidua* (Table 5). The difference in *E* due to the altered $T_a$ response is mainly caused by the additional transpiration at the end of the growing season (Figure 6b). For N13, an increase of 3.7 ± 1.0 (added to 124.8 ± 12.1 kg m$^{-2}$ year$^{-1}$) would be expected if *L. decidua* responded like the trees at S22 (Table 5). Here, the main difference is detected at the beginning of the growing season during colder conditions (Figure 6e). Both the alteration in $R_g$ and *D* response affect *E* less consistently, although N13 *L. decidua* would transpire up to 22.2 ± 1.8 kg m$^{-2}$ year$^{-1}$ more if it had the more gradual *D* response function of S22 *L. decidua* (Table 5).

## 4 | DISCUSSION

Conifers growing at temperature-limited conditions and exposed to shorter growing seasons optimize water transport to facilitate carbon assimilation and use (Körner, 2012; Wieser, 2007). Here, we showed that two conifers commonly occurring at high elevations in Europe apply contrasting strategies in regulating their stomatal conductance ($g_s$), a key mechanism for controlling tree water use dynamics. The analysis of 4 years of sap flow measurements revealed that the pioneer *L. decidua* facilitated higher water conductance (Figure 3), while regulating water loss during atmospheric droughts more tightly than a late-successional species as *P. abies* (Figure 4a). Additionally, the within species ability to adjust their $g_s$ sensitivity to environmental conditions differed between species, where *L. decidua* appeared more plastic (Figure 5c,d).

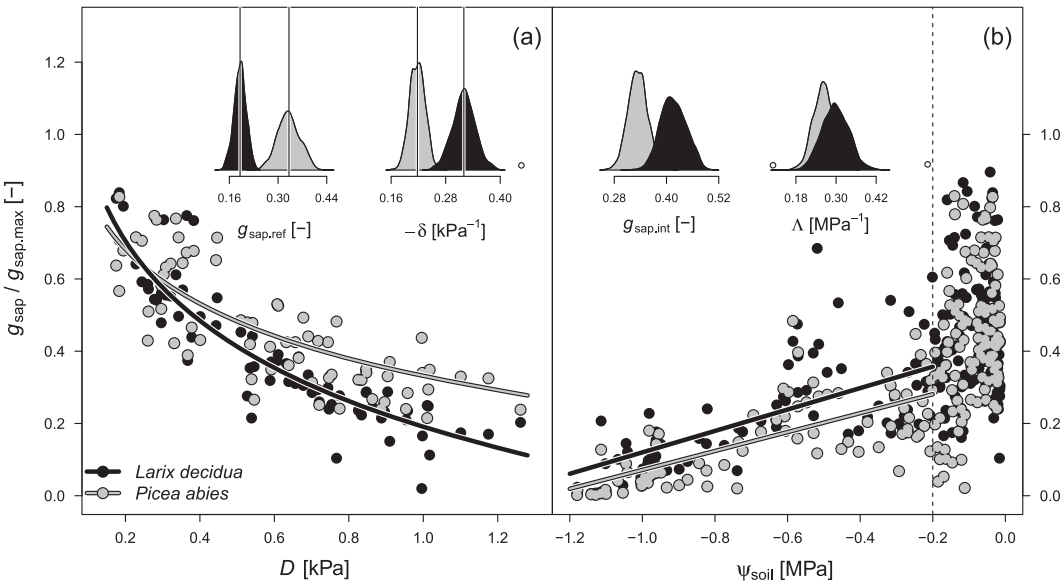


**FIGURE 4** Daily mean standardized crown conductance ($g_{sap}/g_{sap.max}$) for *Larix decidua* and *Picea abies* against *D* and $\psi_{soil}$ at N13, which was the driest site in the study. The species-specific conductance response to *D* (a) and $\psi_{soil}$ (b) are provided. Additionally, we show the Gaussian distribution of the fitted parameters using $\mu$ (mean) and $\sigma$ (standard deviation), derived from the linear-mixed effect model (using the individual as a random factor), and indicate significant difference with lines ($P < 0.05$; using a bootstrap resampling, with $n = 1{,}000$)

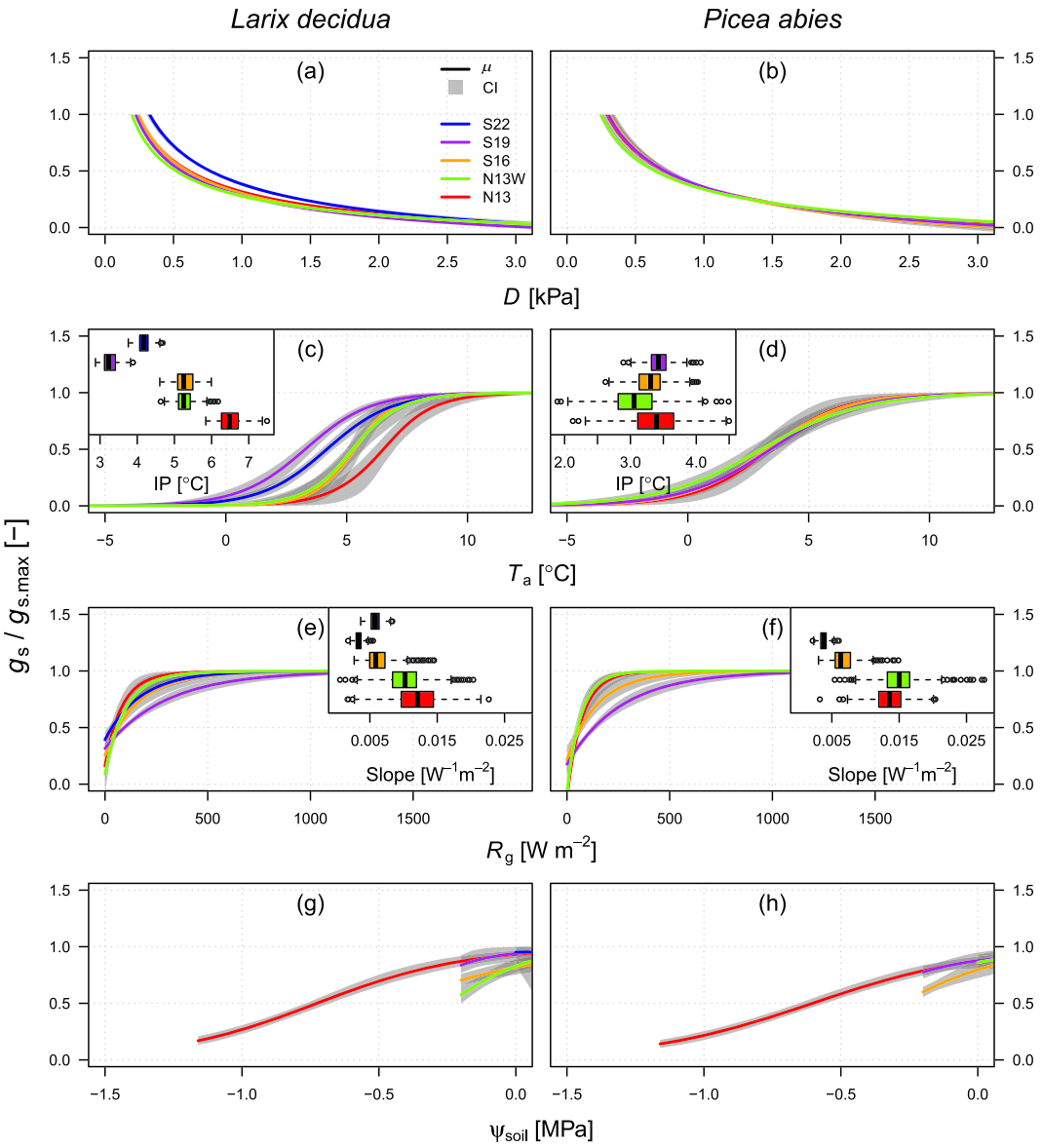


**FIGURE 5** Response functions of the bootstrap boundary-line analysis for *Larix decidua* and *Picea abies* with standardized stomatal conductance ($g_s/g_{s.max}$) fitted against (a, b) vapour pressure deficit (*D*), (c, d) air temperature ($T_a$), (e, f) solar irradiance ($R_g$), and (g, h) soil water potential ($\psi_{soil}$). For $T_a$ (c, d) the inflection points (see the parameter *b* in Table 3), and for $R_g$ (e, f) the slopes (see parameter *a* in Table 3) are presented in the inset boxplots, originating from the 1,000 times bootstrap resampling. The mean (μ) curve and the 95% confidence interval (CI) are provided

## 4.1 | Higher maximum crown and stomatal conductance for *L. decidua* in comparison with *P. abies*

Our study revealed that the two conifers differed in their efficiency to transport water, where *L. decidua* showed a >2 times higher maximum water conductance per unit leaf area (maximum stomatal conductance, $g_{s.max}$) and per unit sapwood area (maximum crown conductance, $g_{sap.max}$) than *P. abies* (Figure 3). The species-specific difference in conductance is highlighted by the higher average transpiration (*E*) for *L. decidua* than for *P. abies* over the 4 years of observations (Figure 2), although *P. abies* is able to reach higher transpiration rates at sites with warmer growing season temperatures (e.g., Wullschleger, Meinzer, & Vertessy, 1998). This species-specific difference in conductance at high elevations was also found by Anfodillo et al. (1998). Yet the steeper increase in $A_S$ with the increasing size (DBH) for *P. abies* (Figure 1) translates to an overall larger leaf area, which compensates for the lower conductance and for larger individuals and even facilitates a higher overall water flux compared to *L. decidua* (see max. $W_u$ in Table 1). Interestingly, no significant increase in maximum conductance with higher elevations was found (Figure 3), although this is commonly reported and attributed to wider tree spacing and more intense radiation (see Körner, 2012). This absence of $g_{s.max}$ plasticity could be attributed to the uncertainty in $A_S$ or $A_L$:$A_S$ values. Yet *P. abies* had consistently higher $A_S$ values and variability compared to *L. decidua*, which is in line with other studies (e.g., Longuetaud, Mothe, Leban, & Mäkelä, 2006; Nawrot, Pazdrowski, & Szymański, 2008; Tyree & Zimmermann, 2002).

Adjusting xylem anatomical properties is an important mechanism for regulating $g_{s.max}$ and could explain species-specific differences in maximum conductance (Klein, 2014; Locosselli & Ceccantini, 2012).

**TABLE 4** Non-linear models used within the boundary-line analysis

| Formula | Spec. | Var. | Site N13 | N13W | S16 | S19 | S22 |
|---|---|---|---|---|---|---|---|
| $g_s/g_{s.max\text{-}D} = a - bD^{-0.5}$ | LD | *a* | −0.347 ± 0.02 | −0.294 ± 0.01 | −0.385 ± 0.02 | −0.361 ± 0.02 | −0.443 ± 0.03 |
| | | *b* | −0.663 ± 0.02 | −0.571 ± 0.01 | −0.685 ± 0.03 | −0.642 ± 0.02 | −0.827 ± 0.03 |
| | PA | *a* | −0.386 ± 0.06 | −0.320 ± 0.02 | −0.450 ± 0.05 | −0.408 ± 0.05 | – |
| | | *b* | −0.743 ± 0.07 | −0.657 ± 0.03 | −0.805 ± 0.06 | −0.764 ± 0.06 | – |
| $g_s/g_{s.max\text{-}Ta} = 1/(1 + e^{-a(Ta - b)})$ | LD | *a* | 0.916 ± 0.29 | 1.012 ± 0.38 | 1.195 ± 0.32 | 0.733 ± 0.10 | 0.729 ± 0.09 |
| | | *b* | 6.480 ± 0.29 | 5.246 ± 0.24 | 5.241 ± 0.24 | 3.239 ± 0.21 | 4.173 ± 0.16 |
| | PA | *a* | 0.650 ± 0.29 | 0.481 ± 0.08 | 0.602 ± 0.08 | 0.558 ± 0.06 | – |
| | | *b* | 3.399 ± 0.40 | 3.051 ± 0.38 | 3.301 ± 0.25 | 3.426 ± 0.17 | – |
| $g_s/g_{s.max\text{-}Rg} = 1 - e^{-a(Rg - b)}$ | LD | *a* | 0.012 ± 0.00 | 0.010 ± 0.00 | 0.006 ± 0.00 | 0.003 ± 0.00 | 0.006 ± 0.00 |
| | | *b* | −12.18 ± 58.68 | −7.48 ± 97.69 | −50.64 ± 35.99 | −115.71 ± 32.25 | −85.76 ± 25.93 |
| | PA | *a* | 0.014 ± 0.00 | 0.015 ± 0.00 | 0.006 ± 0.00 | 0.004 ± 0.00 | – |
| | | *b* | 9.134 ± 9.09 | 5.350 ± 9.20 | −38.56 ± 25.65 | −51.28 ± 23.13 | – |
| $g_s/g_{s.max\text{-}\psi soil} = 1/(1 + a\, e^{(-\psi soil\ b)})$ | LD | *a* | 0.072 ± 0.02 | – | – | – | – |
| | | *b* | 3.654 ± 0.39 | – | – | – | – |
| | PA | *a* | 0.142 ± 0.03 | – | – | – | – |
| | | *b* | 3.239 ± 0.31 | – | – | – | – |

*Note*. For each site and species (LD = *Larix decidua* and PA = *Picea abies*) median and standard deviation of *a* and *b* parameters are provided, as obtained from the bootstrap resampling (*n* = 1,000).

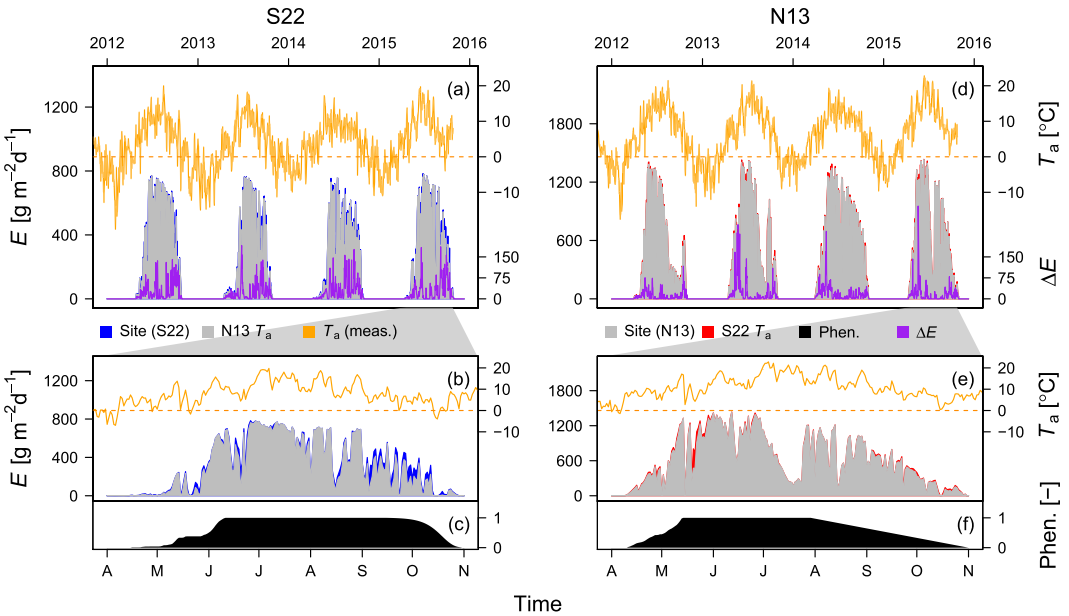


**FIGURE 6** Modelled daily transpiration (*E*) patterns for *Larix decidua* under the climatic conditions of S22 (a–c) and N13 (d–f). Note the different scales of *E* for the S22 and N13 conditions. Response functions presented in Figure 5 are used to model the site response of *E*, where the $T_a$ response was site-specific or exchanged with the response function of the site at the opposite end of the elevational transect. For example, for *L. decidua* growing at S22 the $g_s$-response to $T_a$ would be replaced with the $T_a$ response function observed at N13, resulting in a difference in modelled daily *E* (highlighted in blue in a and b). The difference in *E* induced by the replaced $T_a$ response function is presented with *E* (in g m$^{-2}$ day$^{-1}$; purple lines in a and d). Additionally, mean daily $T_a$ is provided (orange) with the dashed line indicating 0°C. To highlight the differences, a snapshot is provided for the growing season of 2015 for S22 (b) and N13 (c). The modelled *E* was corrected for phenological development, where we corrected *E* for absence (0) to full crown development (1) using a phenological development model (c and f)

The higher $g_{s.max}$ for *L. decidua* could be facilitated by generally wider tracheids compared to *P. abies*, reducing the resistance for water transport up to the crown (Tyree & Zimmermann, 2002) while allowing for lower midday leaf water potentials ($\psi_{leaf}$; Figure S3). According to Hagen–Poiseuille's law (Tyree & Zimmermann, 2002), when assuming a tracheid lumen diameter difference of 30 and 41 μm for *P. abies* and *L. decidua*, respectively (see Carrer, Castagneri, Prendin, Petit, & von Arx, 2017), we find agreement with a three times higher hydraulic conductance for *L. decidua* compared to *P. abies*. Although these findings have to be confirmed with in situ anatomical measurements, they indicate that the xylem structure largely affects the maximum hydraulic conductance. Additionally, xylem density increases with elevation, where narrower tracheids and thicker cell walls help to avoid winter embolism (Mayr, 2007). This results in a decrease in lumen area and may prevent high-elevation conifers from increasing $g_{s.max}$. Otherwise, leaf-related explanations including osmotic adjustments within the stomata might enable *L. decidua* to maintain higher conductance during summer (Badalotti, Anfodillo, & Grace, 2000) or species-specific

**TABLE 5** Modelled transpiration ($E$) considering alternative response functions for air temperature ($T_a$), global irradiance ($R_g$), and vapour pressure deficit ($D$), compared to site-specific response functions

| Species | Site | $E$ (kg m$^{-2}$ year$^{-1}$) | Effect of alternative response function (kg m$^{-2}$ year$^{-1}$) | | |
|---|---|---|---|---|---|
| *Larix decidua* | S22 | 63.7 ± 4.8 | $T_a$ (N13) −5.1 ± 0.7 | $R_g$ (N13) −7.3 ± 0.9 | $D$ (N13) −9.6 ± 1.3 |
| | S19 | 59.7 ± 5.4 | $T_a$ (N13) −4.6 ± 0.7 | $R_g$ (N13) +0.6 ± 0.5 | $D$ (N13) +4.7 ± 1.0 |
| | N13 | 124.8 ± 12.1 | $T_a$ (S22) +3.7 ± 1.0 | $R_g$ (S22) +10.6 ± 0.9 | $D$ (S22) +22.2 ± 1.8 |
| | | | $T_a$ (S19) +4.8 ± 1.3 | $R_g$ (S19) −7.1 ± 2.4 | $D$ (S19) −11.3 ± 0.8 |
| *Picea abies* | S19 | 46.0 ± 4.0 | $T_a$ (N13) +0.4 ± 0.1 | $R_g$ (N13) +0.3 ± 0.4 | $D$ (N13) −0.2 ± 0.1 |
| | N13 | 46.6 ± 6.4 | $T_a$ (S19) −0.3 ± 0.0 | $R_g$ (S19) −2.6 ± 0.6 | $D$ (S19) 0.0 ± 0.1 |

*Note*. As an example, if *Larix decidua* $g_s$-response to $T_a$ for S22 (presented in Figure 5) would be similar to that of N13, then transpiration would have been reduced by 5.1 kg m$^{-2}$ year$^{-1}$. The annual mean and standard deviation of modelled transpiration are provided for the transpiration seasons of 2012–2015 for *L. decidua* and *Picea abies* growing under climatic conditions for S22, S19, and N13. The transpiration season is defined by the sap flow measurements (see Figure 2).

The applied alternative response function for $T_a$, $R_g$ and $D$ of a particular site (presented in brackets) are provided in bold.

differences in leaf traits such as stomatal size and density (Körner et al., 1986; Locosselli & Ceccantini, 2012; Luomala, Laitinen, Sutinen, Kellomäki, & Vapaavuori, 2005).

## 4.2 | Species-specific variations in water use strategies

The exceptional 2015 summer drought, with low soil water potential ($\psi_{soil}$) and high air temperature ($T_a$), caused a cease in transpiration in low elevation *P. abies* (N13; Figure 2d), whereas *L. decidua* showed a strong reduction (Figure 2b). Surprisingly, we found no evidence to support that more drought sensitive *P. abies* would apply a stronger water-saving strategy, by down-regulating conductance to increasing vapour pressure deficit ($D$) stronger than *L. decidua* (Figure 4). The fact that the *P. abies* response function to $D$ is not adjusted to drier growing conditions (e.g., no steeper decrease in $g_s$ with increasing $D$ at the drier site compared to the wet site; Figure 5b) could be explained by the low occurrence of severe droughts within this ecosystem. This is supported by Grossiord et al. (2017) who did not find adjustment of the $g_s$ response to $D$ after 5 years of precipitation reduction in a semi-arid region. On the contrary, *L. decidua* appeared to show a slightly stronger down-regulation with increasing $D$ compared to *P. abies* (Figure 4a), which matches with observations by Oren et al. (1999) and Leo et al. (2014) for *Larix sp*. and *P. abies*. When considering soil drought responses, *P. abies* exhibited consistently lower relative conductance with decreasing $\psi_{soil}$ (or increasing drought; Figure 4b). Yet the slopes of the response of $g_{sap}/g_{sap.max}$ to $\psi_{soil}$ are similar, hinting to the fact that the shallower rooting strategy of *P. abies* versus *L. decidua* is potentially causing less water uptake and storage refilling (Oberhuber, Kofler, Schuster, & Wieser, 2015), instead of a stomatal specific response. This hypothesis is supported by the midday $\psi_{leaf}$ response to decreasing $\psi_{soil}$ (see Figure S3), where the slope of *P. abies* appears to be slightly steeper, although these results are by no means conclusive due to the low number of $\psi_{leaf}$ measurements below a $\psi_{soil}$ of −0.6 MPa ($n$ = 6, $\Delta_{slope}$ = 0.205 MPa$^{-1}$, $P$ = 0.502).

The stronger down-regulation of $g_s$ to $D$ for *L. decidua* could be explained by its larger tracheids being disputably more prone to cavitation during drought episodes (Bouche et al., 2014). Another explanation could be that the thinner cuticula of the deciduous *L. decidua* dehydrates faster and thus initiates stomatal closure faster with higher $D$ (Mayr, 2007). Although our results might be interpreted as *L. decidua* being slightly more isohydric (i.e., more actively regulating stomatal conductance to maintain constant leaf water potential; Klein, 2014) than *P. abies* in mountainous ecosystems, we did find the midday $\psi_{leaf}$ measurements of *L. decidua* to be significantly lower under well-watered conditions ($\Delta_{intercept}$ = 0.235 MPa, $P$ = 0.015; see Figure S3) showing that *L. decidua* might not maintain more constant $\psi_{stem}$. Nevertheless, the more active down-regulation of $g_s$ with increasing $D$ does support that *L. decidua* might be better in maintaining hydraulic functioning under drier growing conditions compared to *P. abies*.

Next to the environmental regulation of $g_s$, a species-specific difference was found in the delay between sap flow diurnal fluctuations and the driving meteorological conditions (due to water storage in the stem; Braun et al., 2010). When comparing start of sap flow and sunrise, we found that *P. abies* sap flow response to sunrise took 1 hr longer compared to *L. decidua*. Interestingly, asynchronous and contrasting tree water use dynamics between co-occurring boreal conifers was also found at the southern limit of the boreal ecozone in central Canada (*Larix laricina* and *Picea mariana*; Pappas et al., 2018) and have been attributed to whole-plant traits trade-offs along the "fast-slow" plant economics spectrum (Reich, 2014). More specifically, the deciduous *Larix* is characterized by a "fast" traits strategy with higher rates of resource acquisition and use, resulting also in higher water conductance whereas the evergreen *Picea* is characterized by a "slow" traits strategy, with lower water conductance (Pappas et al., 2018).

## 4.3 | Plasticity of stomatal conductance to environmental changes

We did not find evidence to support a plastic adjustment of the $g_s$ response to $D$ for *L. decidua* and *P. abies* when growing under persistently different growing season temperatures, as found by Grossiord et al. (2017). When comparing sites across the elevational gradient, only *L. decidua* growing at the treeline site (S22) showed a different

$g_s$ response, with higher conductance below 1.5 kPa (Figure 5a,b). Although the shift in the response function at S22 potentially increases transpiration in the long term by ~10 kg m$^{-2}$ year$^{-1}$ (Table 5), this shift does not appear to relate to increasing elevation or decreasing growing season temperatures (as S19 and S16 show a similar response-function as N13; Figure 5a,b). This lack of apparent plasticity in stomatal response to *D* for high elevation conifers is consistent with Poyatos et al. (2007) who found little evidence for *Pinus sylvestris* L. adjusting the $g_s$ sensitivity to *D* when comparing sites with mean annual temperature ranging from −3.7°C to 9.8°C.

We observed that high elevation conifers adjust their $g_s$ response to $T_a$ (Figure 5c) and $R_g$ (Figure 5e,f) depending on elevation. Surprisingly, only *L. decidua* at higher elevations showed a change in $g_s$ sensitivity to $T_a$ (Figure 5c,d), with a significant inflection point shift of +0.87°C per 1°C increase in mean growing season temperature (May–October). Yet, due to the lack of periods when $g_s$ is not limited by *D* at higher temperatures, we were only able to analyse the $g_s$ response below 13°C. Crop species have shown a similar plasticity in their $g_s$ response to temperature (e.g., Yamori, Noguchi, Hikosaka, & Terashima, 2010), but to our knowledge, few studies focus on $g_s$ sensitivity to temperature for trees (e.g., Drake et al., 2018; Urban, Ingwers, McGuire, & Teskey, 2017) and none have shown its plasticity. In this study, we showed that the observed plasticity of the $g_s$–$T_a$ response enables high-elevation *L. decidua* to transpire up to ~5 kg m$^{-2}$ year$^{-1}$ more (Table 5). In particular, high-elevation *L. decidua* would benefit from this lower operational temperature at the end of the growing season (Figure 6b). At lower elevations, the adjusted $g_s$–$T_a$ response was marginally beneficial in preventing water loss during cold periods at the beginning of the growing season (Figure 6e). Potential reasons for high-elevation *L. decidua* to maintain higher transpiration rates at the end of the growing season include the increase of water transport to facilitate higher carbon assimilation (Wieser, 2007), or the increased facilitation of nutrient transport (Mayr, 2007). More specifically, our results suggest that *L. decidua* employs a more "risky strategy" by sustaining high water conductance under colder conditions, at the cost of losing water at thermal conditions less optimal for photosynthesis (Wieser, 2007) and risking freezing damage (Mayr, 2007). This type of plasticity could be facilitated by changing enzymatic activity that maintains photosynthetic activity and transpiration under less favourable conditions (see Hikosaka, Ishikawa, Borjigidai, Muller, & Onoda, 2006). It could also involve a change in osmotic potential to keep stomata open (Badalotti et al., 2000). We hypothesize that the differences in plasticity of the two species can be explained by the deciduous life strategy of *L. decidua*, with a shorter vegetative season compared to evergreen species, although sap flow measurements for *P. abies* outside the growing season are needed to fully elucidate absolute differences in annual transpiration. Alternatively, pioneers, like *L. decidua*, need to deal with a larger range of environmental conditions, demanding higher maintenance respiration and protection against freezing damage.

Both species showed a weaker down-regulation of $g_s$ to decreasing $R_g$ at higher elevations (Figure 5e,f). This plasticity of the $g_s$–$R_g$ response is likely regulated by an osmotic pressure change within the guard cells, facilitated by specific photoreceptors (Buckley & Mott, 2013). The slower $g_s$ increase with increasing $R_g$ at higher elevations for both species, as well as incomplete stomatal closure at night, could facilitate a faster response to sunrise, thus extending the daily transpiration activity and counteracting the shorter growing season at these mesic sites (Daley & Phillips, 2006). Another possible explanation could be the interplay between $R_g$ and atmospheric $CO_2$ concentration, where the mechanisms to open the guard cells with increasing light change depending upon the $CO_2$ concentration (Buckley & Mott, 2013; Tor-ngern et al., 2014). However, additional measurements are needed to confirm that these patterns are not caused by refilling of xylem and phloem water storage (Matheny et al., 2015; Meinzer, Johnson, Lachenbruch, Mcculloh, & Woodruff, 2009; Zweifel & Häsler, 2001).

G. M. King et al. (2013) revealed a genetically well-mixed population within the Lötschental, supporting our plasticity hypothesis over adaptation. Yet transplantation experiments could aid in further testing this hypothesis, as changes in $g_s$ response to environmental drivers might take a considerable amount of time to become apparent (Livingston & Black, 1987). Notwithstanding, our results show that models estimating evapotranspiration patterns with generalized $g_s$ response functions might underestimate the transpiration amount at high elevations, and potentially high latitudes. A recent modelling study also pinpointed the importance of plant trait plasticity in explaining the recent increase in forest water use efficiency (Mastrotheodoros et al., 2017). Moreover, the vegetation modelling community acknowledges the fundamental role of interspecific and intraspecific plant trait variability in the resulting terrestrial carbon, water, and energy dynamics and the need for trait-based representation of vegetation functioning (Fyllas et al., 2014; Pappas, Fatichi, & Burlando, 2016; Pavlick, Drewry, Bohn, Reu, & Kleidon, 2013; Sakschewski et al., 2015; Scheiter, Langan, & Higgins, 2013). Finally, if we want to fully grasp the effect of climate change on the hydraulic functioning of different tree species, we should move away from focussing on only one hydraulic mechanism (like $g_s$) and apply a more holistic approach, including photosynthetic activity, the tree's water storage capacity, and wood anatomical structure (e.g., Egea, Verhoef, & Luigi, 2011; Köcher, Horna, & Leuschner, 2013). Such information would improve the parameterization of terrestrial ecosystem models and would result in more constrained predictions of the water, carbon, and energy dynamics under changing environmental conditions.

## ACKNOWLEDGEMENTS

We thank Gregory King, Roger Köchli, Daniel Nievergelt, and Anne Verstege for their aid in the extensive fieldwork and labwork performed throughout the past years at the Lötschental transect. We also would like to thank David C. Frank, Flurin Babst, Niklaus E. Zimmermann, Rafael Wüest Karpati, and Damaris Zurell for discussion. This work was funded by a Swiss National Science Foundation project (SNSF), LOTFOR (150205). C. P. acknowledges support from the Stavros Niarchos Foundation, the ETH Zurich Foundation, and the SNSF (grants P2EZP2_162293, P300P2 174477).

## ORCID

*Richard L. Peters* https://orcid.org/0000-0002-7441-1297
*Christoforos Pappas* https://orcid.org/0000-0001-5721-557X
*Georg von Arx* https://orcid.org/0000-0002-8566-4599
*Elisabeth Graf Pannatier* https://orcid.org/0000-0003-2676-2583
*Patrick Fonti* https://orcid.org/0000-0002-7070-3292

## REFERENCES


Allen, C. D., Macalady, A. K., Chenchouni, H., Bachelet, D., Mcdowell, N., Vennetier, M., … Cobb, N. (2010). A global overview of drought and heat-induced tree mortality reveals emerging climate change risks for forests. *Forest Ecology and Management*, *259*, 660–684. https://doi.org/10.1016/j.foreco.2009.09.001

Anderegg, W. R. L., Klein, T., Bartlett, M., Sack, L., Pellegrini, A. F. A., Choat, B., & Jansen, S. (2016). Meta-analysis reveals that hydraulic traits explain cross-species patterns of drought-induced tree mortality across the globe. *Proceedings of the National Academy of Sciences*, *113*, 5024–5029. https://doi.org/10.1073/pnas.1525678113

Anfodillo, T., Rento, S., Carraro, V., Furlanetto, L., Urbinati, C., & Carrer, M. (1998). Tree water relations and climatic variations at the alpine timberline: Seasonal changes of sap flux and xylem water potential in *Larix decidua* Miller, *Picea abies* (L.) Karst. and *Pinus cembra* L. *Annals of Forest Science*, *55*, 159–172. https://doi.org/10.1051/forest:19980110

Arneth, A., Kelliher, F. M., Bauer, G., Hollinger, D. Y., Byers, J. N., Hunt, J. E., … Schulze, E. (1996). Environmental regulation of xylem sap flow and total conductance of *Larix gmelinii* trees in eastern Siberia. *Tree Physiology*, *16*, 247–255. https://doi.org/10.1093/treephys/16.1-2.247

Badalotti, A., Anfodillo, T., & Grace, J. (2000). Evidence of osmoregulation in *Larix decidua* at alpine treeline and comparative responses to water availability of two co-occurring evergreen species. *Annals of Forest Science*, *57*, 623–633. https://doi.org/10.1051/forest:2000146

Bannister, P., & Neuner, G. (2001). Frost resistance and the distribution of Conifers. In F. J. Bigras, & S. J. Colombo (Eds.), *Conifer cold hardiness. pp. 3–21. Tree physiology* ( ed., Vol. 1). Dordrecht: Springer. https://doi.org/10.1007/978-94-015-9650-3_1

Barigah, T. S., Ibrahim, T., Bogard, A., Faivre-Vuillin, B., Lagneau, L. A., Montpied, P., & Dreyer, E. (2006). Irradiance-induced plasticity in the hydraulic properties of saplings of different temperate broad-leaved forest tree species. *Tree Physiology*, *26*, 1–11.

Beniston, M. (2003). Climatic change in mountain regions: A review of possible impacts. *Climatic Change*, *59*, 5–31.

Bonan, G. B. (2008). Forests and climate change: Climate benefits of forests. *Science*, *320*, 1444–1450. https://doi.org/10.1126/science.1155121

Bouche, P. S., Larter, M., Domec, J., Burlett, R., Gasson, P., Jansen, S., & Delzon, S. (2014). A broad survey of hydraulic and mechanical safety in the xylem of conifers. *Journal of Experimental Botany*, *65*, 4419–4431. https://doi.org/10.1093/jxb/eru218

Boyer, J. S. (1967). Leaf water potential measure with a pressure chamber. *Plant Physiology*, *42*, 133–137. https://doi.org/10.1104/pp.42.1.133

Braun, S., Schindler, C., & Leuzinger, S. (2010). Use of sap flow measurements to validate stomatal functions for mature beech (*Fagus sylvatica*) in view of ozone uptake calculations. *Environmental Pollution*, *158*, 2954–2963. https://doi.org/10.1016/j.envpol.2010.05.028

Brodribb, T. J., Mcadam, S. A. M., Jordan, G. J., & Martins, S. C. V. (2014). Conifer species adapt to low-rainfall climates by following one of two divergent pathways. *Proceedings of the National Academy of Sciences*, *111*, 14489–14493. https://doi.org/10.1073/pnas.1407930111

Buckley, T. N., & Mott, K. A. (2013). Modelling stomatal conductance in response to environmental factors. *Plant, Cell & Environment*, *36*, 1691–1699. https://doi.org/10.1111/pce.12140

Burger, H. (1953). Holz, Blattmenge und Zuwachs. *XII: Fichten im gleichaltrigen Hochwald. Mitt. Schweiz. Mitteilungen der Schweizerischen Anstalt für das Forstliche Versuchswesen*, *29*, 38–130.

Carrer, M., Castagneri, D., Prendin, A. L., Petit, G., & von Arx, G. (2017). Retrospective analysis of wood anatomical traits reveals a recent extension in tree cambial activity in two high-elevation conifers. *Frontiers in Plant Science*, *8*, 1–13.

Chambers, J. L., Hinckley, T. M., & Hinckley, T. M. (1985). Boundary-line analysis and models of leaf conductance for four oak-hickory forest species. *Forest Science*, *31*, 437–450.

Cordell, S., Goldstein, G., Mueller-Dombois, D., Webb, D., & Vitousek, P. M. (1998). Physiological and morphological variation in *Metrosideros polymorpha*, a dominant Hawaiian tree species, along an altitudinal gradient: The role of phenotypic plasticity. *Oecologia*, *113*, 188–196. https://doi.org/10.1007/s004420050367

Daley, M. J., & Phillips, N. G. (2006). Interspecific variation in nighttime transpiration and stomatal conductance in a mixed New England deciduous forest. *Tree Physiology*, *26*, 411–419. https://doi.org/10.1093/treephys/26.4.411

Damour, G., Simonneau, T., Cochard, H., & Urban, L. (2010). An overview of models of stomatal conductance at the leaf level. *Plant, Cell & Environment*, *33*, 1419–1438.

Day, M. E. (2000). Influence of temperature and leaf-to-air vapor pressure deficit on net photosynthesis and stomatal conductance in red spruce (*Picea rubens*). *Tree Physiology*, *20*, 57–63. https://doi.org/10.1093/treephys/20.1.57

De Schepper, V., & Steppe, K. (2010). Development and verification of a water and sugar transport model using measured stem diameter variations. *Journal of Experimental Botany*, *61*, 2083–2099. https://doi.org/10.1093/jxb/erq018

Delpierre, N., Dufrêne, E., Soudani, K., Ulrich, E., Cecchini, S., Boé, J., & François, C. (2009). Modelling interannual and spatial variability of leaf senescence for three deciduous tree species in France. *Agricultural and Forest Meteorology*, *149*, 938–948. https://doi.org/10.1016/j.agrformet.2008.11.014

Drake, J. E., Tjoelker, M. G., Vårhammer, A., Medlyn, B. E., Reich, P. B., Leigh, A., … Barton, C. V. M. (2018). Trees tolerate extreme heatwave via sustained transpirational cooling and increased leaf thermal tolerance. *Global Change Biology*, *24*, 2390–2402. https://doi.org/10.1111/gcb.14037

Egea, G., Verhoef, A., & Luigi, P. (2011). Towards an improved and more flexible representation of water stress in coupled photosynthesis-stomatal conductance models. *Agricultural and Forest Meteorology*, *151*, 1370–1384. https://doi.org/10.1016/j.agrformet.2011.05.019

Ellenberg, H., & Leuschner, C. (2010). *Vegetation Mitteleuropas mit den Alpen in ökologischer, dynamischer und historischer Sicht*. Stuttgart, Germany: Ulmer.

Esper, J., & Schweingruber, F. H. (2004). Large-scale treeline changes recorded in Siberia. *Geophysical Research Letters*, *31*, 1–5.

Farjon, A., & Filer, D. (2013). *An atlas of the world's conifers: an analysis of their distribution, biogeography, diversity and conservation status*. United Kingdom: BRILL.

Fatichi, S., Leuzinger, S., & Körner, C. (2014). Moving beyond photosynthesis: From carbon source to sink-driven vegetation modeling. *New Phytologist*, *201*, 1086–1095. https://doi.org/10.1111/nph.12614

Fyllas, N. M., Gloor, E., Mercado, L. M., Sitch, S., Quesada, C. A., Domingues, T. F., … Lloyd, J. (2014). Analysing Amazonian forest productivity using a new individual and trait-based model (TFS v.1). *Geoscientific Model Development*, *7*, 1251–1269. https://doi.org/10.5194/gmd-7-1251-2014

Gelman, A., & Hill, J. (2007). *Data analysis using regression and multilevel/hierarchical models*. Cambridge, United Kingdom: Cambridge University Press.

Gower, S. T., & Richards, J. H. (1990). Larches: Deciduous conifers in an evergreen world. *Bioscience*, *40*, 818–826. https://doi.org/10.2307/1311484

Granier, A. (1985). Une nouvelle méthode pour la mesure du flux de sève brute dans le tronc des arbres. *Annals of Forest Science*, *42*, 193–200. https://doi.org/10.1051/forest:19850204

Granier, A., Bréda, N., Biron, P., & Villette, S. (1999). A lumped water balance model to evaluate duration and intensity of drought constraints in forest stands. *Ecological Modeling*, *116*, 269–283. https://doi.org/10.1016/S0304-3800(98)00205-1

Granier, A., & Loustau, D. (1994). Measuring and modelling the transpiration of a maritime pine canopy from sap-flow data. *Agricultural*

*and Forest Meteorology*, *71*, 61–81. https://doi.org/10.1016/0168-1923(94)90100-7

Grossiord, C., Sevanto, S., Borrego, I., Chan, A. M., Collins, A. D., Dickman, L. T., … Mcdowell, N. G. (2017). Tree water dynamics in a drying and warming world. *Plant, Cell & Environment*, *40*, 1861–1873. https://doi.org/10.1111/pce.12991

Hetherington, A., & Woodward, I. (2003). The role of stomata in sensing and driving environmental change. *Nature*, *424*, 901–908. https://doi.org/10.1038/nature01843

Hikosaka, K., Ishikawa, K., Borjigidai, A., Muller, O., & Onoda, Y. (2006). Temperature acclimation of photosynthesis: Mechanisms involved in the changes in temperature dependence of photosynthetic rate. *Journal of Experimental Botany*, *57*, 291–302. https://doi.org/10.1093/jxb/erj049

IPCC (2013). *Climate change 2013: The physical science basis. Contribution of working group I to the fifth assessment report of the intergovernmental panel on climate change*, by. Cambridge, United Kingdom and New York: T. F. S. Cambridge University Press.

Jarvis, P. G. (1976). The interpretation of the variations in leaf water potential and stomatal conductance found in canopies in the field. *Philosophical Transactions of the Royal Society of London. Series B, Biological Sciences*, *273*, 593–610. https://doi.org/10.1098/rstb.1976.0035

Ježík, M., Blaženec, M., Letts, M. G., Ditmarová, Ľ., Sitková, Z., & Střelcová, K. (2015). Assessing seasonal drought stress response in Norway spruce (*Picea abies* (L.) Karst.) by monitoring stem circumference and sap flow. *Ecohydrology*, *386*, 378–386.

Katul, G. G., Palmroth, S., & Oren, R. (2009). Leaf stomatal responses to vapour pressure deficit under current and CO2-enriched atmosphere explained by the economics of gas exchange. *Plant, Cell and Environment*, *32*, 968–979. https://doi.org/10.1111/j.1365-3040.2009.01977.x

Kelliher, M., Leuning, R., & Schulze, D. (1993). Evaporation and canopy characteristics of coniferous forests and grasslands. *Oecologia*, *95*, 153–163. https://doi.org/10.1007/BF00323485

King, G., Fonti, P., Nievergelt, D., Büntgen, U., & Frank, D. (2013). Climatic drivers of hourly to yearly tree radius variations along a 6°C natural warming gradient. *Agricultural and Forest Meteorology*, *168*, 36–46. https://doi.org/10.1016/j.agrformet.2012.08.002

King, G. M., Gugerli, F., Fonti, P., & Frank, D. C. (2013). Tree growth response along an elevational gradient: Climate or genetics? *Oecologia*, *173*, 1587–1600. https://doi.org/10.1007/s00442-013-2696-6

Klein, T. (2014). The variability of stomatal sensitivity to leaf water potential across tree species indicates a continuum between isohydric and anisohydric behaviours. *Functional Ecology*, *28*, 1313–1320. https://doi.org/10.1111/1365-2435.12289

Klein, T., Yakir, D., Buchmann, N., & Grünzweig, J. M. (2014). Towards an advanced assessment of the hydrological vulnerability of forests to climate change-induced drought. *New Phytologist*, *201*, 712–716. https://doi.org/10.1111/nph.12548

Köcher, P., Horna, V., & Leuschner, C. (2013). Stem water storage in five coexisting temperate broad-leaved tree species: Significance, temporal dynamics and dependence on tree functional traits. *Tree Physiology*, *33*, 817–832. https://doi.org/10.1093/treephys/tpt055

Körner, C. (2012). *Alpine treelines: Functional ecology of the global high elevation tree limits*. Basel, Switzerland: Springer.

Körner, C., Bannister, P., & Mark, A. F. (1986). Altitudinal variation in stomatal conductance, nitrogen content and leaf anatomy in different plant life forms in New Zealand. *Oecologia*, *69*, 577–588. https://doi.org/10.1007/BF00410366

Körner, C., & Paulsen, J. (2004). A world-wide study of high altitude treeline temperatures. *Journal of Biogeography*, *31*, 713–732. https://doi.org/10.1111/j.1365-2699.2003.01043.x

Leo, M., Oberhuber, W., Schuster, R., Grams, T. E. E., Matyssek, R., & Wieser, G. (2014). Evaluating the effect of plant water availability on inner alpine coniferous trees based on sap flow measurements. *European Journal for Forest Research*, *133*, 691–698. https://doi.org/10.1007/s10342-013-0697-y

Lin, Y., Medlyn, B. E., Duursma, R. A., Prentice, I. C., Wang, H., Baig, S., … Windgate, L. (2015). Optimal stomatal behaviour around the world. *Nature Climate Change*, *5*, 459–464. https://doi.org/10.1038/nclimate2550

Lindroth, A. (1985). Canopy conductance of coniferous forests related to climate. *Water Resources Research*, *21*, 297–304. https://doi.org/10.1029/WR021i003p00297

Lintunen, A., Paljakka, T., Jyske, T., Peltoniemi, M., Sterck, F., Von Arx, G., … Hölttä, T. (2016). Osmolality and non-structural carbohydrate composition in the secondary phloem of trees across a latitudinal gradient in Europe. *Frontiers in Plant Science*, *7*. https://doi.org/10.3389/fpls.2016.00726

Livingston, N. J., & Black, T. A. (1987). Stomatal characteristics and transpiration of three species of conifer seedlings planted on a high elevation south-facing clear-cut. *Canadian Journal of Forest Research*, *17*, 1273–1282. https://doi.org/10.1139/x87-197

Lockhart, J. A. (1965). An analysis of irreversible plant cell elongation. *Journal of Theoretical Biology*, *8*, 264–275. https://doi.org/10.1016/0022-5193(65)90077-9

Locosselli, G. M., & Ceccantini, G. (2012). Plasticity of stomatal distribution pattern and stem tracheid dimensions in *Podocarpus lambertii*: An ecological study. *Annals of Botany*, *110*, 1057–1066. https://doi.org/10.1093/aob/mcs179

Longuetaud, F., Mothe, F., Leban, J., & Mäkelä, A. (2006). *Picea abies* sapwood width: Variations within and between trees. *Scandinavian Journal of Forest Research*, *21*, 41–53.

López, R., López De Heredia, U., Collada, C., Cano, F. J., Emerson, B. C., Cochard, H., & Gil, L. (2013). Vulnerability to cavitation, hydraulic efficiency, growth and survival in an insular pine (*Pinus canariensis*). *Annals of Botany*, *111*, 1167–1179. https://doi.org/10.1093/aob/mct084

Lu, P., Urban, L., & ZHao, P. (2004). Granier's thermal dissipation probe (TDP) method for measuring sap flow in trees: Theory and practice. *Acta Botanica Sinica*, *46*, 631–646.

Luomala, E., Laitinen, K., Sutinen, S., Kellomäki, S., & Vapaavuori, E. (2005). Stomatal density, anatomy and nutrient concentrations of Scots pine needles are affected by elevated CO2. *Plant, Cell and Environment*, *28*, 733–749.

Martínez-Vilalta, J., Cochard, H., Mencuccini, M., Sterck, F., Herrero, A., Korhonen, J. F. J., … Zweifel, R. (2009). Hydraulic adjustment of Scots pine across Europe. *New Phytologist*, *184*, 353–364. https://doi.org/10.1111/j.1469-8137.2009.02954.x

Maseyk, K. S., Lin, T., Rotenberg, E., Grünzweig, J. M., Schwartz, A., & Yakir, D. (2008). Physiology-phenology interactions in a productive semi-arid pine forest. *New Phytologist*, *178*, 603–616. https://doi.org/10.1111/j.1469-8137.2008.02391.x

Mastrotheodoros, T., Pappas, C., Molnar, P., Burlando, P., Keenan, T. F., Gentine, P., … Fatichi, S. (2017). Linking plant functional trait plasticity and the large increase in forest water use efficiency. *Journal of Geophysical Research – Biogeosciences*, *122*, 2393–2408. https://doi.org/10.1002/2017JG003890

Matheny, A. M., Bohrer, G., Garrity, S. R., Morin, T. H., Howard, C. J., & Vogel, C. S. (2015). Observations of stem water storage in trees of opposing hydraulic strategies. *Ecosphere*, *6*, 1–13.

Mayr, S. (2007). Limits in water relations. In G. Wieser, & M. Tausz (Eds.), *Trees at their upper limit* (pp. 145–162). Berlin Heidelberg: Springer. https://doi.org/10.1007/1-4020-5074-7_8

Mayr, S., Hacke, U., Schmid, P., Schienbacher, F., & Gruber, A. (2006). Frost drought in conifers at the alpine timberline: Xylem disfunction and adaptations. *Ecology*, *87*, 3175–3185. https://doi.org/10.1890/0012-9658(2006)87[3175:FDICAT]2.0.CO;2

Meier, E. S., Lischke, H., Schmatz, D. R., & Zimmermann, N. E. (2012). Climate, competition and connectivity affect future migration and ranges of European trees. *Global Ecology and Biogeography*, *21*, 164–178. https://doi.org/10.1111/j.1466-8238.2011.00669.x

Meinzer, F. C., Johnson, D. M., Lachenbruch, B., Mcculloh, K. A., & Woodruff, D. R. (2009). Xylem hydraulic safety margins in woody plants: Coordination of stomatal control of xylem tension with hydraulic capacitance. *Functional Ecology*, *23*, 922–930. https://doi.org/10.1111/j.1365-2435.2009.01577.x

Meinzer, F. C., Woodruff, D. R., Eissenstat, D. M., Lin, H. S., Adams, T. S., & McCulloh, K. A. (2013). Above- and belowground controls on water use by trees of different wood types in an eastern US deciduous forest. *Tree Physiology*, *33*, 345–356. https://doi.org/10.1093/treephys/tpt012

Mencuccini, M. (2003). The ecological significance of long-distance water transport: Short-term regulation, long-term acclimation and the hydraulic costs of stature across plant life forms. *Plant, Cell and Environment*, *26*, 163–182. https://doi.org/10.1046/j.1365-3040.2003.00991.x

Monteith, J. L. (1965). Evaporation and environment. *Symposia of the Society for Experimental Biology*, *19*, 205–234.

Monteith, J. L., & Unsworth, M. (2013). *Principles of environmental physics, fourth*. Oxford, UK: Academic Press.

Moser, L., Fonti, P., Büntgen, U., Esper, J., Luterbacher, J., Franzen, J., & Frank, D. (2010). Timing and duration of European larch growing season along altitudinal gradients in the Swiss Alps. *Tree Physiology*, *30*(2),225–233.

Murray, M. B., Cannell, M. G. R., & Smith, R. I. (1989). Date of budburst of fifteen tree species in Britain following climatic warming. *Journal of Applied Ecology*, *26*, 693–700. https://doi.org/10.2307/2404093

Myneni, R. B., Dong, J., Tucker, C. J., Kaufmann, R. K., Kauppi, P. E., Liski, J., … Hughes, M. K. (2001). A large carbon sink in the woody biomass of Northern forests. *Proceedings of the National Academy of Sciences*, *98*, 14784–14789. https://doi.org/10.1073/pnas.261555198

Nawrot, M., Pazdrowski, W., & Szymański, M. (2008). Dynamics of heartwood formation and axial and radial distribution of sapwood and heartwood in stems of European larch (*Larix decidua* Mill .). *Journal of Forest Science*, *54*, 409–417. https://doi.org/10.17221/30/2008-JFS

Nobel, P. S. (2009). *Physicochemical and environmental plant physiology*. United Kingdom, Oxford: Elsevier Inc.

Oberhuber, W., Kofler, W., Schuster, R., & Wieser, G. (2015). Environmental effects on stem water deficit in co-occurring conifers exposed to soil dryness. *International Journal of Biometeorology*, *417–426*, 417–426.

Oren, R., Sperry, J. S., Katul, G. G., Pataki, D. E., Ewers, B. E., Phillips, N., & Schäfer, K. V. R. (1999). Survey and synthesis of intra- and interspecific variation in stomatal sensitivity to vapour pressure deficit. *Plant, Cell & Environment*, *22*, 1515–1526. https://doi.org/10.1046/j.1365-3040.1999.00513.x

Pappas, C., Fatichi, S., & Burlando, P. (2016). Modeling terrestrial carbon and water dynamics across climatic gradients: Does plant trait diversity matter? *New Phytologist*, *209*, 137–151. https://doi.org/10.1111/nph.13590

Pappas, C., Matheny, A. M., Baltzer, J. L., Barr, A., Black, T. A., Bohrer, G., … Stephens, J. (2018). Boreal tree hydrodynamics: Asynchronous, diverging, yet complementary. *Tree Physiology*, *00*, 1–12.

Pavlick, R., Drewry, D. T., Bohn, K., Reu, B., & Kleidon, A. (2013). The Jena Diversity-Dynamic Global Vegetation Model (JeDi-DGVM): A diverse approach to representing terrestrial biogeography and biogeochemistry based on plant functional trade-offs. *Biogeosciences Discussions*, *9*, 4627–4726. https://doi.org/10.5194/bgd-9-4627-2012

Peters, R. L., Fonti, P., Frank, D. C., Poyatos, R., Pappas, C., Kahmen, A., … Steppe, K. (2018). Quantification of uncertainties in conifer sap flow measured with the thermal dissipation method. *The New Phytologist*, *219*, 1283–1299. https://doi.org/10.1111/nph.15241

Peters, R. L., Klesse, S., Fonti, P., & Frank, D. C. (2017). Contribution of climate vs. larch budmoth outbreaks in regulating biomass accumulation in high-elevation forests. *Forest Ecology and Management*, *401*, 147–158. https://doi.org/10.1016/j.foreco.2017.06.032

Phillips, N., & Oren, R. (1998). Comparison of daily representations of canopy conductance based on two conditional time-conductance on environmental factors. *Annals of Forest Science*, *55*, 217–235.

Poyatos, R., Martínez-Vilalta, J., Čermák, J., Ceulemans, R., Granier, A., Irvine, J., … Mencuccini, M. (2007). Plasticity in hydraulic architecture of Scots pine across Eurasia. *Oecologia*, *153*, 245–259. https://doi.org/10.1007/s00442-007-0740-0

Price, D. T., & Black, T. A. (1989). Estimation of forest transpiration and C0 2 uptake using the Penman-Monteith equation and a physiological photosynthesis model. In T. A. Black, D. L. Spittlehouse, M. D. Novak, & D. T. Price (Eds.), *Estimation of areal evapotranspiration*, *Publ. No*. (Vol. 177) (pp. 213–228). Wallingford, UK: Int. Assoc. Hydrol. Sci.

R development core team (2013). *R: A language and environment for statistical computing*. Vienna, Austria: R Foundation of Statistical Computing.

Reich, P. B. (2014). The world-wide "fast-slow" plant economics spectrum: A traits manifesto. *Journal of Ecology*, *102*, 275–301. https://doi.org/10.1111/1365-2745.12211

Rigling, A., Bigler, C., Eilmann, B., Feldmeyer-Christe, E., Gimmi, U., Ginzler, C., … Dobbertin, M. (2013). Driving factors of a vegetation shift from Scots pine to pubescent oak in dry alpine forests. *Global Change Biology*, *19*, 229–240. https://doi.org/10.1111/gcb.12038

Roman, D. T., Novic, K. A., Brzostek, E. R., Dragoni, D., Rahman, F., & Phillips, R. P. (2015). The role of isohydric and anisohydric species in determining ecosystem-scale response to severe drought. *Oecologia*, *179*, 641–654. https://doi.org/10.1007/s00442-015-3380-9

Rossi, S., Deslauriers, A., Seo, J., Rathgeber, C. B. K., Anfodillo, T., Morin, H., … Jalkanen, R. (2008). Critical temperatures for xylogenesis in conifers of cold climates. *Global Ecology and Biogeography*, *17*, 696–707. https://doi.org/10.1111/j.1466-8238.2008.00417.x

Sakschewski, B., von Bloh, W., Boit, A., Rammig, A., Kattge, J., Poorter, L., … Thonicke, K. (2015). Leaf and stem economics spectra drive diversity of functional plant traits in a dynamic global vegetation model. *Global Change Biology*, *21*, 2711–2725. https://doi.org/10.1111/gcb.12870

Scheiter, S., Langan, L., & Higgins, S. I. (2013). Next-generation dynamic global vegetation models: Learning from community ecology. *New Phytologist*, *198*, 957–969. https://doi.org/10.1111/nph.12210

Schulla, J. (2015). Model description WaSiM completely revised version of 2012 with 2013 to 2015 extensions. In J. Schulla (Eds.), *Technical Report: Hydrology Software Consulting* (p. 332). Zürich, Switzerland.

Shatar, T. M., & McBratney, A. B. (2004). Boundary-line analysis of field-scale yield response to soil properties. *Journal of Agricultural Science*, *142*, 553–560. https://doi.org/10.1017/S0021859604004642

Soja, A. J., Tchebakova, N. M., French, N. H. F., Flannigan, M. D., Shugart, H. H., Stocks, B. J., … Stackhouse, P. W. Jr. (2007). Climate-induced boreal forest change: Predictions versus current observations. *Global and Planetary Change*, *56*, 274–296. https://doi.org/10.1016/j.gloplacha.2006.07.028

Steltzer, H., & Post, E. (2009). Seasons and life cycles. *Science*, *324*, 886–888. https://doi.org/10.1126/science.1171542

Sultan, S. E. (2000). Phenotypic plasticity for plant development, function and life history. *Trends in Plant Science*, *5*, 537–542.

Tatarinov, F., Rotenberg, E., Maseyk, K., Ogée, J., Klein, T., & Yakir, D. (2016). Resilience to seasonal heat wave episodes in a Mediterranean pine forest. *New Phytologist*, *210*, 485–496. https://doi.org/10.1111/nph.13791

Teepe, R., Dilling, H., & Beese, F. (2003). Estimating water retention curves of forest soils from soil texture and bulk density. *Journal of Plant Nutrition and Soil Science*, *166*, 111–119. https://doi.org/10.1002/jpln.200390001

Tor-ngern, P., Oren, R., Ward, E. J., Palmroth, S., Mccarthy, H. R., & Domec, J. (2014). Rapid report increases in atmospheric CO2 have little influence on transpiration of a temperate forest canopy. *New Phytologist*, *205*, 518–525.

Tuzet, A., Perrier, A., & Leuning, R. (2003). A coupled model of stomatal conductance, photosynthesis. *Plant, Cell and Environment*, *26*, 1097–1116. https://doi.org/10.1046/j.1365-3040.2003.01035.x

Tyree, M. T., & Zimmermann, M. (2002). *Xylem structure and the ascent of sap*. New York, USA: Springer. https://doi.org/10.1007/978-3-662-04931-0

Urban, J., Ingwers, M. W., McGuire, M. A., & Teskey, R. O. (2017). Increase in leaf temperature opens stomata and decouples net photosynthesis from stomatal conductance in *Pinus taeda* and *Populus deltoids x nigra*. *Journal of Experimental Botany*, *68*, 1757–1767. https://doi.org/10.1093/jxb/erx052

Valladares, F., Matesanz, S., Guilhaumon, F., Araújo, M. B., Balaguer, L., Benito-Garzón, M., … Zavala, M. A. (2014). The effects of phenotypic plasticity and local adaptation on forecasts of species range shifts under climate change. *Ecology Letters*, *17*, 1351–1364. https://doi.org/10.1111/ele.12348

van Genuchten, M. T. (1980). A closed-form equation for predicting the hydraulic conductivity of unsaturated soils. *Soil Science Society of America Journal*, *44*, 892–898. https://doi.org/10.2136/sssaj1980.03615995004400050002x

Walthert, L., & Meier, E. S. (2017). Tree species distribution in temperate forests is more influenced by soil than by climate. *Ecology and Evolution*, *7*, 9473–9484. https://doi.org/10.1002/ece3.3436

Wieser, G. (2007). Limitation by insufficient carbon assimilation and allocation. In G. Wieser, & M. Tausz (Eds.), *Trees at their upper limit—Treelife limitation at the alpine timberline* (pp. 79–129). Dordrecht, The Netherlands: Springer. https://doi.org/10.1007/1-4020-5074-7_6

Wieser, G., Leo, M., & Oberhuber, W. (2014). Transpiration and canopy conductance in an inner alpine Scots pine (Pinus sylvestris L.) forest. *Flora*, *209*, 491–498. https://doi.org/10.1016/j.flora.2014.06.012

WMO (2008). *Guide to meteorological instruments and methods of observation, appendix 4B, WMO-No. 8 (CIMO Guide)*. Geneva, Switzerland: World Meteorological Organization.

Wullschleger, S. D., Meinzer, F. C., & Vertessy, R. A. (1998). A review of whole-plant water use studies in trees. *Tree Physiology*, *18*, 499–512. https://doi.org/10.1093/treephys/18.8-9.499

Yamori, W., Noguchi, K., Hikosaka, K., & Terashima, I. (2010). Phenotypic plasticity in photosynthetic temperature acclimation among crop species with different cold tolerances. *Plant Physiology*, *152*, 388–399. https://doi.org/10.1104/pp.109.145862

Zimmermann, N. E., Edwards, T. C. Jr., Graham, C. H., Pearman, P. B., & Svenning, J. C. (2010). New trends in species distribution modelling. *Ecography*, *33*, 985–989. https://doi.org/10.1111/j.1600-0587.2010.06953.x

Zweifel, R., & Häsler, R. (2001). Dynamics of water storage in mature subalpine *Picea abies*: Temporal and spatial patterns of change in stem radius. *Tree Physiology*, *21*, 561–569. https://doi.org/10.1093/treephys/21.9.561

## SUPPORTING INFORMATION

Additional supporting information may be found online in the Supporting Information section at the end of the article.

**How to cite this article:** Peters RL, Speich M, Pappas C, et al. Contrasting stomatal sensitivity to temperature and soil drought in mature alpine conifers. *Plant Cell Environ*. 2019;42: 1674–1689. https://doi.org/10.1111/pce.13500